Overexpression of DnaJ chaperones in ameliorating toxicities associated with FUS and TDP-43

Snehal Ahire[1], Tania Bose[1, #]

1: Dept. of Biotechnology, with jointly merged Institute of Bioinformatics and Biotechnology (IBB), Savitribai Phule Pune University, Ganeshkhind, Pune 411007, India

#: corresponding author (ORCID 0000-0002-5478-0407)

Email: tania.bose@gmail.com; tbose@unipune.ac.in (Tania Bose, corresponding author)

Abstract

Amyotrophic Lateral Sclerosis (ALS) is an adult-onset neurodegenerative disease. It primarily affects the motor neurons, leading to muscle weakness and eventual death of patients. Various factors, such as genetics, environment, age, etc, are involved in the etiopathogenesis of ALS. As ALS is a highly challenging and complex disease that involves various pathogeneses linked with progressive motor neuron degeneration, it is difficult to have a single therapeutic target against this disease. ALS mutants of TDP-43 and FUS are showing slow growth as well as protein aggregation in the cytoplasm in yeast. Our study involves cloning of 38 *Drosophila* DnaJ domain chaperones and overexpressing them in a yeast ALS model. After the interaction of mutants TDP-43 and FUS with the DnaJ domain chaperones, they were categorized into suppressors and enhancers. The major hits on our screen were CG7872, Hsc70-4, and Mrj, which rescued TDP-43 toxicity by reducing the protein aggregation and slow growth in yeast cells. In the FUS, slow growth and protein aggregation is reduced with the chaperones CG32641 and CG6693, resulting in a lowering of the FUS toxicity. On the other hand, chaperones CG2911, CG2790, and CG8476 in the presence of TDP-43 overexpression, grow more slowly with increasing punctae in yeast cells. These chaperones increase the toxicity of

TDP-43. Similarly, in FUS, Hsc20, CG7130, CG2911, and JdpC also showed a slow growth phenotype and increased protein aggregation in yeast cells. These chaperones enhance the toxicity of FUS.

This screening will enhance our understanding of ALS, and the chaperones identified in this study can serve as neuroprotective agents for ALS.

Keywords: neurodegenerative disease, TDP-43, FUS, yeast, ALS, DnaJ domain chaperones, Hsp40, ALS, RNA binding proteins

1.0 Introduction

ALS involves an interplay of different epigenetic genes associated with its pathogenesis. These genes include SOD1, FUS, TARDBP, VAPB, VCP, and OPTN [1–4]. These genes are found in all types of pathophysiology associated with ALS. ALS is found in two forms: sporadic and familial. ALS also results from family history and lifestyle factors, including smoking and dietary factors [5,6].

In ALS, RNA processing pathways and RNA-binding proteins are involved in the etiopathogenesis [7,8]. The genes involved in disease conditions of ALS, TDP-43, and FUS have RNA-binding domains, and after mutation, both these genes are found to be toxic in multiple studies. In 2006, Arai and Newmann found TDP-43 to be an essential component of ubiquitinated protein aggregates in FTLD-U and sporadic ALS[9]. In ALS, when TDP-43 is derived from the damaged central nervous system, toxic TDP-43 is found in hyperphosphorylated form, cleaved to obtain a C-terminal fragment, and ubiquitinated [10]. FUS also exhibits ubiquitous expression, similar to TDP-43, and its expression is independent. After the missense mutation, FUS also forms cytoplasmic aggregates in neurons [11]. In 0.4% of familial ALS cases, FUS/TLS mutations were found [11,12]. Though TDP-43 and FUS have

RNA-binding domains and the same cytoplasmic aggregation properties, their toxicity mechanism differs subtly [13].

Previous studies show that positive inclusion, i.e., protein aggregation, was found in mutant SOD-1 ALS cases [14]. Protein aggregation is due to the protein quality control system (PQC) failure to handle folding and the missed degradation of misfolded protein [15]. Protein aggregation is not toxic in every case. Sometimes, protein aggregation can be a protective storage mechanism. However, inside the cell, the location of protein aggregates and the size of the aggregates can be considered toxic [12].

Neurodegenerative diseases like ALS, Alzheimer's, Huntington's, and Parkinson's have a protein aggregation trait, a specific protein that can fold into an alternative stable form, leading to protein aggregation and accumulation as fibrillar deposits in tissues [17–19].

In our study, we have used the yeast model to focus on the mechanism of cellular toxicity and aggregation phenotype in both TDP-43 and FUS [13,20,21].

Chaperones are the proteins that assist in the folding or unfolding of large proteins and differentiate between misfolded proteins, unfolded proteins, and aggregated proteins with specific biological functions [22]. The main cellular function of the chaperones is assisting in the quality control of protein folding. Not all chaperones can prevent aggregation. Some chaperones assist in restoring correct folding and denatured protein function and aid in the assembly and disassembly of proteins. They also help fold *de-novo* proteins and, in the translocation and disaggregation of protein aggregates [23]. Chaperones are classified into five main families based on their molecular mass and sequence similarities [24].

In this study, we used *Drosophila* DnaJ domain chaperones, i.e., Hsp40, which is also called DnaJ co-chaperone. They are the proteins that help chaperones assist in protein folding. These non-client-binding molecules help to fold the proteins by binding Hsp70 or Hsp90, or both. Co-chaperones can induce or inhibit the ATP hydrolysis activity of Hsp70 and Hsp90

chaperones [25]. They bring about conformational changes in chaperones or modify the substrate and contribute to the chaperone's function [23]. There are 100 different co-chaperones in mammals, many of which follow the categories based on their domain architecture [26]. Most of them are classified into two groups: J domain proteins and tetracopeptide repeats, i.e., TPR [27]. Together, chaperones and cochaperones form a network. To modulate their function, each can identify a subset of misfolded proteins as a substrate and interact with other chaperones and cochaperones [27].

In prokaryotes and eukaryotes, Heat shock proteins (HSPs) are ubiquitously conserved for the survival of stressful conditions like heat stress [28]. It can cause harmful damage to cellular architecture and interfere with vital cellular functions. To combat heat stress, the cell activates its classical pathway, whereby it expresses heat shock proteins for a shorter period for cell survival and maintains protein homeostasis [29].

Our observation supports enhanced and rescued protein aggregation and cellular growth by the interaction of DnaJ domain chaperones with ALS mutants. We found potential suppressors and enhancers with the interaction of DnaJ domain chaperones. To check our findings, we expressed 38 DnaJ domain chaperones from flies in yeast [30,31].

Multiple studies have shown that heat shock proteins and chaperones help to reduce the toxicity of mutant TDP-43 as well as FUS. In HEK293 cells, overexpression of HSF-1/DNAJB21/HSP70 shows reduced cytoplasmic protein aggregation caused by mutant TDP-43 [32]. Previous work has shown that HSP40 chaperone Sis1 plays a role in the folding of proteins, the transport of misfolded proteins, as well as the catabolism of ubiquitin-dependent misfolded proteins. When Sis1 is overexpressed in TDP-43 cells, it lowers the toxicity of TDP-43. Its mammalian homolog, DnaJB1, when overexpressed in rodent primary cortex, also lowers TDP-43 toxicity in neurons [33]. In the HeLa cell line, it was observed that HSP70

99 prevents amyloid aggregation caused by the mutant TDP-43 and prevents the liquid-to-solid
100 transition [34].
101 TDP-43 and FUS both undergo liquid-to-solid phase separation [35,36]. This process results in
102 liquid-like sections forming in the cytoplasm during stress and at the site of DNA damage. The
103 pHSP 40 chaperones Hdj2 (DNAJA1) and Hdj1 (DNAJB1) assist FUS in undergoing phase
104 separation. Additionally, Hdj1 aids the phase-separated FUS in inhibiting amyloid and protein
105 aggregation within the cell. The small heat shock protein Hsp27 is co-localized with FUS and
106 prevents their phase separation by binding FUS to the low complexity region, thereby helping
107 to avoid the formation of stress granules in the cell model [37].
108 Gitler and colleagues established yeast as a model to study ALS related to TDP-43 [20]. The
109 same group also reported using yeast for genome-wide screening of FUS to uncover the
110 mechanisms of the cellular pathways and the genes involved in FUS toxicity [13]. Taking cues
111 from these studies, we explore the interactions between TDP-43 and FUS with Drosophila
112 DnaJ domain chaperones, including their potential suppressors and enhancers.
113 Our study emphasizes protein aggregation and cellular toxicity in ALS mutants, involving the
114 overexpression of TDP-43 and FUS genes. We screened 38 DnaJ domain chaperones of
115 *Drosophila*. which includes: CG30156, CG5001, Mrj, DnaJ60, CG2911, CG6693, JdpC,
116 CG9828, CG4164, CG2887, CG12020, JdpA, CG10565, Tpr2, Csp, CG7394, CG7130,
117 CG8476, CG7872, Hsc20, Sec63, P58IPK, CG43322, CG7133, CG7556, CG14650, CG32641,
118 CG11035, CG10375, CG17187, DnaJ1, CG3061, CG8531 and CG7387. These include Hsc70
119 (Hsc70-1, Hsc70-4) and Hsp70 chaperones (Hsp70Aa and Hsp70Bb). We chose only those
120 chaperones that play a role in protein folding listed in **Table 2**. Their function and activity are
121 the same as the human homologs [38,39].
122 We found that chaperones CG7872, Mrj, and Hsc70 suppress the toxicity of TDP-43, and
123 chaperones CG32641 and CG6693 suppress the toxicity of FUS.

These chaperones, found to play a protective role in other disease conditions as well.

DNAJC25 is an orthologue of CG7872, localized in the cytoplasm, and has a role in hepatocarcinoma suppressor [40] Mrj is present ubiquitously in the cytosol. A mutation in DNAJB6 caused frontotemporal dementia and limb-girdle muscular dystrophy type 1 case of the patient's brain sample [41]. It was also found that DNAJB6 inhibits polyQ aggregation and increases the life span in polyQ mice [42]. *Drosophila* Mrj helps Orb2 to reduce its prion conversion and also helps to reduce Htt aggregates [31]. In Parkinson's disease, DNAJB6 with cochaperones Hsp70 reduces the α-synuclein aggregation [43] Both Huntington's and Parkinson's disease have been found that Mrj suppress the toxicity of Htt and α-synuclein disease-causing proteins, but no such evidence has been found in the ALS-causing gene TDP-43. Also, Hsc70 is a co-chaperone of DnaJ domain chaperones and is also found to improve the TDP-43 toxicity in sporadic ALS patients [44,45]. *Drosophila* Hsc70-4 has a human orthologue of HSPA8 and is found in multiple studies in where it is involved in the clearance of misfolded proteins [46,47]

DNAJC9 is a human orthologue of CG6693 and has been found to play a role in cancer [48]. DNAJC9 also takes part in histone chaperone function with the help of the cochaperone Hsp70 [49]. DNAJB9 is also a human orthologue of chaperone CG32641 and is found associated with ER degradation machinery, and also interacts with CFTR and rescues the cystic fibrosis-causing gene Δ F508 [50,51]

Some chaperones can also enhance the toxic phenotype, specifically slow growth and protein aggregation in both mutant FUS and TDP-43. We found that chaperones CG2911, CG2790, and CG8476 are enhancers of TDP-43 toxicity, while chaperones Hsc20, CG2911, CG7130, and JDPC enhance FUS toxicity. Previously, they were also found to contribute to toxicity in certain disease conditions[52–55].

149

150

151 To develop TDP-43 and FUS models in *Saccharomyces cerevisiae,* we used galactose-
152 inducible plasmids pRS426 Gal-TDP-43-GFP and pAG416 GalFUS-YFP, respectively. Mutant
153 TDP-43 and FUS show slow growth and protein aggregation in yeast cells at permissive
154 temperature, while the same time control shows normal growth and cytoplasmic diffusion.
155 When these two mutants, expressed with 38 DnaJ domain chaperones, we found that some
156 chaperones suppressed the toxicity while some chaperones enhanced the toxicity of the
157 respective mutant, TDP-43 and FUS.

158

159 **2.0 Results**

160 **2.1 Yeast model of TDP-43 and FUS: growth assay and cytoplasmic aggregation**

161 We made TDP-43 and FUS yeast models from the TDP-43 and FUS plasmids pRS426 Gal-
162 TDP-43-GFP and pAG416 Gal-FUS-YFP, respectively. This construct has a Ura marker with
163 a GFP tag on the C-terminal and a galactose-inducible promoter. **(Supplementary Fig S1)**

164 The TDP-43 mutant results in slow growth and protein aggregation in yeast cells, indicating
165 pathogenicity [20]. Similarly, the FUS mutant also shows slow growth and protein aggregation,
166 indicating pathogenicity in yeast cells [13].

167 We used an empty vector as a control, and TDP-43 and FUS for determining ALS toxicity
168 [57,58]. The spot dilution assay of TDP-43 and FUS mutants shows slow growth compared to
169 the control in Gal-Ura. **(Supplementary Fig S2a)**

170 A quantitative study of both mutants was done using a 48-hour growth assay. TDP-43 and FUS
171 cultures were added in triplicate in a 96-well plate at 30°C with orbital shaking. Growth assay
172 of TDP-43 and FUS also showed a slowdown of TDP-43 and FUS growth in liquid medium,
173 i.e, Gal-Ura, compared to the control. **(Supplementary Fig S2b)**

174 We further checked whether our mutants show protein aggregation under confocal microscopy.
175 For the microscopy, cultures were inoculated in SD-Ura, and on the following day, after a
176 raffinose wash was given and 20% Galactose was added. We find two morphologies in confocal
177 microscopy: diffused cytoplasm and punctae. In TDP-43 and FUS, we find more punctae,
178 indicating protein aggregation in the yeast cell, and in the control, we found a cytoplasmic
179 diffusion, which indicates no protein aggregation in the cell. **(Supplementary Fig S2c)**
180 As the TDP-43 and FUS mutant strains show a slow growth phenotype and aggregation of
181 proteins compared to the control, we further checked these mutants against 38 DnaJ domain
182 chaperones. We further screened the DnaJ domain chaperones and cochaperones to
183 check whether they show slow or rescue growth and their aggregation properties.
184

185 **2.2 Enhancers and suppressors of TDP-43 and FUS w.r.t *Drosophila* DnaJ domain**
186 **chaperones based on growth assay**

187 We transformed 38 DnaJ domain chaperones with our ALS mutants, TDP-43 and FUS. These
188 transformed colonies of DnaJ domain chaperones were selected and inoculated in the SD-Trp-
189 Ura medium. On the second day, cultures were spotted onto SD-Trp-Ura and SGal-Trp-Ura
190 plates. SD-Trp-Ura is a control, and SGal-Trp-Ura serves as a test. Chaperones that enhance
191 the mutation effect are collectively called enhancers. In SGal-Trp-Ura plates, chaperones
192 CG2911, CG2790, and CG8476 grow more slowly than the control luciferase; they are
193 enhancers of TDP-43 toxicity (**Fig. 1a).** Whereas chaperones grow better in SGal-Trp-Ura
194 plates than in control, i.e., luciferase. These chaperones are enhancers of FUS (**Fig. 1f).**
195 Chaperones that made the ALS mutant grow better in SGal-Trp-Ura plates than the control,
196 i.e., luciferase suppresses the effect of the ALS mutation, and are referred to as a suppressor.
197 Chaperones Mrj, Hsc70-4, and CG7872 are suppressors of TDP-43 toxicity (**Fig.1a)** and in
198 SD-Trp-Ura they serve as control **(Supplementary Fig. S4).** Chaperones CG5001(previously

199 published) [30]. CG6693 and CG32641 grow better in SGal-Trp-Ura plates than luciferase.
200 These chaperones are suppressors of FUS toxicity (**Fig. 1f).** In SD-Trp-Ura plates show no
201 effect **(Supplementary Fig. S5).**
202 To quantify the growth effect, we did a 48-hour growth curve assay of DnaJ chaperones on
203 TDP-43 and FUS mutants. TDP-43 and FUS transformants were inoculated in an SD-Trp-Ura
204 medium for primary culture. The next day, O.D. was adjusted, and 20% galactose was added.
205 Cultures were added in triplicate in 96 96-well plate and placed in a Biotek Epoch
206 spectrophotometer for 48 hrs at 30^0C for occasional shaking. The data obtained from this
207 experiment were processed in GraphPad Prism 8.0. Similar to the spot dilution assay,
208 This 48-hour growth curve shows a growth difference compared to the luciferase.
209 Chaperones CG2911, CG2790, and CG8476 grow slower than luciferase in a 48-hour growth
210 curve. This indicates that these chaperones enhance the toxicity of mutant TDP-43. Chaperones
211 Mrj, Hsc70, and CG7872 grow better than luciferase, suggesting these chaperones rescue TDP-
212 43 toxicity (**Fig. 1 b)**.
213 In FUS, chaperones Hsc20, CG2911, CG7130, and JDPC with the FUS mutant grow slower
214 compared to luciferase. This indicates that these chaperones enhance the toxicity of FUS. Co-
215 expression of FUS with the chaperones CG6693 and CG5001 (previously published) has been
216 shown to rescue the slow growth phenotype. (**Fig.1g).** SD-Trp-Ura shows no effect
217 **(Supplementary Fig. S5)**
218 For the classification of the enhancers and suppressors of DnaJ domain chaperones in the 48-
219 hour growth curve, we calculated the area under the curve based on the values of the 48-hour
220 growth curve. The area under the curve values were normalized with luciferase. A graph was
221 plotted in GraphPad prism 8.0. Positive values of chaperones on the right-hand side are
222 considered suppressors. The negative values of chaperones on the left-hand side are called
223 enhancers (**Fig. 1c and 1h).**

224 **2.3 Classification of weak enhancers and no effect on *Drosophila* DnaJ domain chaperone**
225 **based on growth.**

226 DnaJ domain chaperones of *Drosophila* were screened to see the effect on ALS mutant TDP-
227 43 and FUS, after the yeast transformation of ALS mutants with DnaJ domain chaperones and
228 Co-chaperones. Initially, we checked by using a serial dilution assay. Positive clones were
229 selected from the transformation and inoculated in SD-Trp-Ura (dextrose, YNB, and
230 Tryptophan and Uracil lacking medium) [14,20]. After 48 hrs, serially diluted cultures were
231 spotted on SGal-Trp-Ura and SD-Trp-Ura plates. Plates with dextrose (SD) serve as a control
232 **(Supplementary Fig. S4 and S5)**, while galactose plates are the test and were observed for
233 growth, as ALS plasmids have galactose-inducible promoters.

234 To quantify the effect of mutants on DnaJ domain chaperones, we did 48 hrs growth curve
235 assay. ALS mutant TDP-43 and FUS with control luciferase and transformed chaperones were
236 subjected to induced 20% galactose. These were grown at 30°C for 48 hrs, and the $O.D._{600}$ nm
237 was measured every 30 minutes. Using 3 biological independent replicates, graphs were plotted
238 in GraphPad Prism 8.0 software. In (**Fig.2),** the red line shows the mutants with transformed
239 DnaJ domain chaperones, and the blue line shows the growth curve of ALS mutants with an
240 empty vector. ($n=3$, $P<0.05$, paired t-test).

241 The area under the curves is calculated for each chaperone, including luciferase converted into
242 logarithmic values. Each value was further normalized with luciferase. A graph was plotted in
243 GraphPad Prism 8.0 software. Chaperones that grow slower with ALS mutants were aligned to
244 the right-hand side with a positive value were called suppressors, and the chaperones that are
245 aligned to the left-hand side with a negative value are called enhancers (**Fig.2c and 2f).** The
246 classification of enhancers and suppressors of other chaperones is based on the values of the
247 growth curve from the area under the curve.

248 In spot dilution assay and 48 hrs growth curve of TDP-43, chaperones CG12020, CG7394,
249 CG4164, DnaJ60, CG3061, Hsp70Aa, CG32641, DnaJ1, JdpC, CG2887, Hsc20 and JdpA,
250 grow less compared to Luciferase. These are classified as weak enhancers. Other chaperones
251 like CG14650, Tpr2, CG9828, CG7556, P58IPK, and Hsp70Bb grow equally to Luciferase and
252 show no effect on the growth (n=3, $P<0.05$, paired t-test) shown in (**Fig. 2a).**
253 In spot dilution assay and 48 hrs growth curve of FUS, chaperones CG9828, CG12020,
254 Hsp70Aa, Hsp70Bb, CG11035, CG3061, DnaJ60, CG7133, CG14650, CG2887, CG10375
255 grow less compared to luciferase, classified weak enhancer. Whereas chaperones CG7556,
256 CG17187, CG43322, Csp, Sec63, CG11035, and Hsc70-1 show no effect on growth in the
257 48-hr growth curve (**Fig. 2f).**

258 In the area under the curve of TDP-43, chaperones CG10565, CG12020, CG3061, DnaJ1,
259 CG2911, CG7133, CG4164, DnaJ60, Droj1, and CG7394, JdpA, and JdpC are aligned to the
260 left-hand side. These are classified as weak enhancers. Whereas chaperones CG14650, Tpr2,
261 CG9828, CG7556, P58IPK, and Hsp70Bb show no significant effect on growth. They are
262 either aligned to the right-hand side or left-hand side and may be classified as intermediate.

263 In the area under the curve of FUS, chaperones CG9828, CG12020, Hsp70Aa, Hsp70Bb,
264 CG11035, CG3061, DnaJ60, CG7133, CG14650, CG2887, and CG10375 are aligned to the
265 left-hand side and assigned a negative value. These are called weak enhancers. Chaperones
266 CG7556, CG17187, CG43322, Csp, Sec63, CG11035, P58IPK, and Hsc70-1 show no effect
267 on growth in the 48-hour growth curve. They are aligned either to the left-hand side or the
268 right-hand side. Therefore, they are classified as having no effect.
269 The area under the curve of these chaperones shows results in (**Fig.2c and 2h).**
270

271 **2.4 Enhancers and suppressors of ALS mutant TDP-43 and FUS based on protein**
272 **aggregation in *S. cerevisiae***

273 Transformants of TDP-43 and FUS were induced with 20% galactose to express the ALS gene.
274 Under a confocal microscope, GFP expression is observed in yeast cells [20]. TDP-43 and FUS
275 showed puncta, a sign of protein aggregation, and the control showed diffused cytoplasm with
276 no protein aggregation inside the cell.
277 Around 100-150 cells were counted for ALS mutant TDP-43, FUS, and control independently.
278 These were scored for the percentage of punctae and diffused cytoplasm. Representative
279 images are shown in (**Fig.1d and i).** Based on confocal images, cells were classified into two
280 types: cells with diffused cytoplasm and cells with punctae, and compared to mutants with
281 empty vector, luciferase. The graph was plotted in GraphPad Prism. Chaperones, when
282 overexpressed with a mutant, have a more cytoplasmic diffusion than punctae compared to the
283 empty vector. These chaperones are termed suppressors of the mutation. Those chaperones that
284 showed more punctae than diffused cytoplasm were classified as enhancers. Chaperones Mrj,
285 Hsc70-4, and CG7872 suppressed the effect of the mutation, and chaperones CG2911,
286 CG2790, and CG8476 enhanced the mutation of TDP-43 in ALS. Shown in (**Fig.1e)**.
287 Chaperones CG5001(previously published) and CG6693 suppressed the effect of FUS toxicity,
288 and chaperones Hsc20, CG2911, CG7130, and JDPC enhanced the FUS toxicity in yeast cells.
289 Shown in (**Fig. 1i**).
290

291 **2.5 Classification of weak enhancers and no effect. Based on protein aggregation in TDP-**
292 **43 and FUS**

293 To check the protein aggregation of FUS and TDP-43 with the DnaJ domain chaperone, live
294 cell imaging was done. Transformed cultures were inoculated in an SD-Trp-Ura medium
295 (Dextrose, YNB, and Trp-Ura dropout). 20% galactose induction was given. The next day,
296 microscopy was done. Chaperones that show more diffused cytoplasm than punctae are called
297 suppressors, and chaperones CG10565, CG12020, CG3061, DnaJ1, CG2911, CG7133,

298 CG4164, DnaJ60, Droj1, and CG7394, JdpA, and JdpC that show more punctae than diffused
299 cytoplasm are called enhancers.
300 Microscopic images of TDP-43 with chaperones CG14650, Tpr2, CG9828, CG7556, P58IPK,
301 and Hsp70Bb have more punctae compared to luciferase. Chaperones are showing a mixed
302 phenotype **(Fig.2d)**
303 Microscopic images of FUS with chaperones CG9828, CG12020, Hsp70Aa, Hsp70Bb,
304 CG11035, CG3061, DnaJ60, CG7133, CG14650, CG2887, and CG10375 are showing punctae
305 than luciferase. Chaperones CG7556, CG17187, CG43322, Csp, Sec63, CG11035, P58IPK,
306 and Hsc70-1 showing mixed phenotype (**Fig.2i).**
307 For the quantitation of microscopic data, 100 cells were counted. Punctae and diffused
308 cytoplasm were counted for each transformant, and average values were plotted in GraphPad
309 prism. The graph shows puncta are more than diffused cytoplasm in each DnaJ domain
310 chaperone. Shown in both FUS (**Fig. 2j)** and TDP-43 (**Fig.2e).**
311 Chaperones of TDP-43, CG12020, CG7394, CG4164, DnaJ60, CG3061, Hsp70Aa, CG32641,
312 DnaJ1, JdpC, CG2887, Hsc20 and JdpA have a higher percentage of punctae than diffused
313 cytoplasm. Chaperones CG14650, Tpr2, CG9828, CG7556, P58IPK and Hsp70Bb are showing
314 a mixed phenotype
315 Chaperones of FUS CG9828, CG12020, Hsp70Aa, Hsp70Bb, CG11035, CG3061, DnaJ60,
316 CG7133, CG14650, CG2887, and CG10375 have more percentage of punctae compared to
317 luciferase. Chaperones CG7556, CG17187, P58IPK, CG43322, Csp, Sec63, CG11035,
318 CG10565 and Hsc70-1 shows mixed phenotype.
319
320
321
322

TDP-43		FUS	
Weak enhancer	**No effect**	**Weak enhancer**	**No effect**
CG12020	CG14650	CG9828	CG7556
CG7394	Tpr2	CG12020	CG17187
CG4164	CG7556	Hsp70Aa	P58IPK
Dnaj60	CG9828	Hsp70Bb	Csp
CG3061	Hsp70Bb	CG11035	Sec63
Hsp70Aa	P58IPK	CG3061	CG43322
CG32641		Dnaj60	CG11035
DnaJ1		CG7133	Hsc70-1
JdpC		CG3061	CG10565
CG2887		CG14650	
Hsc20		CG2887	
JDPA		CG10375	

Table 1. list of enhancers and no effect chaperones on ALS mutant TDP-43 and FUS

343 **3.0 Discussion**

344 RNA-binding proteins TDP-43 and FUS play a role in ALS pathogenesis. Both have some
345 structural similarities, including the presence of an RNA-binding domain and a prion-like
346 domain. They are both mutated in ALS [8,59].

347 Although they have certain structural similarities, both genes contribute independently to ALS
348 pathogenesis [60]

349 As per Arai and Newmann 2006, TDP-43 is localized in the nucleus and later spreads out to
350 form cytoplasmic aggregates in ALS and FTLD patients [9,10] .

351 Yeast cells do not have a true TDP-43 homolog but have RNA-binding proteins of similar
352 domain architecture. TDP-43 might aggregate and sequester these proteins, which will offset
353 their normal function [[61].

354 In Parkinson's, Huntington's, Alzheimer's, and prion-related studies, the respective protein
355 forms, intracellular aggregates, and toxicity in yeast cells. Similarly, TDP-43 also forms
356 cytoplasmic aggregates and can be added to the list of human misfolding diseases of proteins
357 [62].

358 FUS also forms cytoplasmic aggregates in neurons after a missense mutation [11]. FUS is
359 normally located in the nucleus. After mutation, FUS forms pathogenic aggregates in motor
360 neurons [63]

361 Pure forms of TDP-43 and FUS also form cytoplasmic aggregates in multiple studies of yeast
362 [20,21,64]. In animals and cellular models ATX2 gene is found to contribute to TDP-43 toxicity
363 and ALS pathogenesis. It is a polyglutamine protein, and the human orthologue of yeast is also
364 found mutated in spinocerebellar ataxia type 2 [65]. Furthermore, it was observed that TDP-43
365 and ATX2 are associated in a complex [64]. In yeast, the pure form of the TDP-43 gene in vitro
366 can form multiple aggregates in vivo. Additionally, a pure TDP-43 aggregates assay aids in
367 identifying small molecules and cellular factors capable of impeding or reversing TDP-43

aggregates [21]. After dissecting the TDP-43 and expressing it in yeast, it was noticed that the C-terminal and RNA recognition motif contribute to TDP-43 toxicity [20].

Yeast is a genetically tractable model, and it is possible to reiterate multiple features of TDP-43 pathology in yeast [62].This includes screening of multiple genomes for modifiers of protein aggregation and their toxicity. This is one of the approaches that can be used to pursue effective diagnosis and treatment [20].

In our observations, TDP-43 and FUS mutants showed slow growth in yeast cells after spot dilution, indicating cellular stress [[13,20]. After 24 hours of galactose induction, these mutants show protein aggregates in the cell under the microscope.

Screening of these mutants with 38 DnaJ domain chaperones showed that some chaperones enhanced and some chaperones reduced the mutants' toxicity in ALS. We labelled them as enhancers and suppressors of the respective mutants, i.e, TDP-43 and FUS.

By screening *Drosophila* DnaJ domain chaperones, we found that chaperones CG7872, Mrj, and Hsc70-4 can rescue the toxicity of mutant TDP-43. HSc70-1 can also rescue the toxic phenotype of TDP-43, but not better like Hsc70-4 and CG32641 and CG6693 rescuing the toxicity of mutant FUS. Also, in our previous findings, CG5001 rescues both the mutants TDP-43 and FUS [30]. In human Hsp70, chaperones also found DNAJAs, DNAJBs, and DNAJCc chaperones rescue the toxicity of TDP-43 in ALS [66].

Also, chaperone CG5001(previously published) is a common suppressor in TDP-43 and FUS, and from our observation, chaperone CG2911 is a common enhancer in both TDP-43 and FUS. Chaperones CG7872, Hsc70-4, and Mrj demonstrate a more significant growth effect in mutant TDP-43. In the spot dilution assay and the growth curve, they grow comparatively better than the control. In microscopy, they exhibit a greater prevalence of the diffused cytoplasm phenotype than punctae; hence, we refer to them as suppressors of TDP-43.

It was found that Mrj's human orthologue is DNAJB6, known for its potent anti-aggregation effect in mouse models [42]. DNAJC25 is an ortholog of CG7872, belonging to the HSP40 family C, and plays a role in various human diseases, including neurodegenerative disorders[67]. Cochaperone Hsc70 influences TDP-43 toxicity in ALS patients[44]

Hsc70-4 is the human orthologue of HPSA8 and has been found in multiple studies of autophagy-related work[68][47] Previously, it was also found it prevent necroptosis initiation and bind to reverse RIP3 amyloid in mammalian cell culture[69]

In the case of mutant FUS, chaperones CG32641 and CG6693 are suppressors. Because they show more growth than luciferase in both spot dilution and growth curve. Microscopic quantitation shows more of the diffused cytoplasmic morphology and fewer punctae in the cell. Therefore, they are referred to as suppressors of FUS toxicity.

From previous studies, it is known that DNAJC9 is the human orthologue of CG6693 and is associated with cervical cancer. It is probably upregulated by reducing or protecting against apoptosis in the cancer cell line [70]. One more study in the zebrafish model stated that DNAJC9 acts in the downstream regulating pathway of the tumor suppressor gene p53 [71].

Also, CG32641 has a DNAJB9 human orthologue and is known for its ER-associated degradation machinery [50]. In the mouse model, it was found that it rescues the cystic fibrosis-causing gene Δ F508, and also directly interacts with CFTR [51].

From this study of Drosophila DnaJ domain chaperones, we also discovered certain enhancers that exacerbate the toxic phenotype, specifically slow growth and protein aggregation in both mutant FUS and TDP-43. Chaperones CG2911, CG2790, and CG8476 enhance TDP-43 toxicity and have also been shown to be toxic in multiple studies. DNAJC21 is the human orthologue of CG2790, and its mutation is associated with bone marrow failure and cancer[72].

Meanwhile, DNAJB9 is the human orthologue of CG8476, whose normal function involves protein folding. It is predominantly active in the endoplasmic reticulum and is found in the miR-32 gene in myeloid acute leukaemia [55].

Whereas, chaperones Hsc20, CG2911, CG7130, and JDPC are found to be enhancers of mutant FUS. They also have a role in other disorders like Hsc20 is also a mitochondrial chaperone, and its human orthologue is HSCB; its mutation in *Drosophila* larvae causes reduced iron-sulphur cluster enzyme activity[54]. JdpC has a human orthologue to DNAJC12, and in whole-exome sequencing, it is found responsible for hyperphenylalaninemia and global developmental delay in some children [53].

CG2911 is a common enhancer found in both TDP-43 and FUS, and its human orthologue is DNAJC24, and malignancy is never been reported before recently, it was reported it involved in hepatocellular carcinoma [52]. In our case, it also shows toxicity when overexpressed in both the mutant TDP-43 and FUS.

We found in the screening of the TDP-43 background that chaperones CG12020, CG7394, CG4164, DnaJ60, CG3061, Hsp70Aa, CG32641, DnaJ1, JdpC, CG2887, Hsc20 and JdpA are weak enhancers. This may be due to the reason that in the growth and spot dilution assay, these chaperones grow more slowly compared to the control. In microscopy, we find more punctae in the cytoplasm than luciferase. Accordingly, we labelled them as weak enhancers as shown in the **Table.1 (Fig. 2a, b**, **c, and e)**.

In the FUS strains, chaperones CG9828, CG12020, Hsp70Aa, Hsp70Bb, CG11035, CG3061, DnaJ60, CG7133, CG14650, CG2887, and CG10375 are weak enhancers. Their growth and spot dilution assay show slower growth compared to luciferase. Also, in microscopy, they show more puncta than luciferase. In a graph of area under the curve, they are aligned on the left-hand side, and in microscopic quantitation, they show more puncta. Therefore, they are classified as weaker enhancers of FUS toxicity as shown in **Table.1** (**Fig.2f, g, h, and i).**

Some chaperones do not show any significant change in the toxicity of mutant TDP-43 example, CG14650, Tpr2, CG9828, CG7556, P58IPK, and Hsp70Bb. Spot dilution and growth curve estimation show equal growth. It is difficult to conclude whether they are enhancers or suppressors.

Similarly, in mutant FUS also some chaperones, CG7556, CG17187, P58IPK, CG43322, Csp, Sec63, CG11035, CG10565, and Hsc70-1 do not show significant effects in spot dilution and growth curve. From these data, it is difficult to conclude whether these chaperones have any effect on FUS toxicity.

In our study, we used *Drosophila* DnaJ domain chaperones in a yeast background to look for potential suppressors and enhancers in both TDP-43 and FUS. Also, we find suppressors and enhancers that were previously unknown in ALS.

Based on the *Drosophila* DnaJ domain chaperones screening with these two mutants, we find that chaperone CG7872 reduces the toxicity of TDP-43 in yeast cells, which is previously unknown. There are many studies on Mrj, which show that it reduces the toxic aggregation in Huntington's and Parkinson's disease [31,42,43]. Based on our findings, we think Mrj possibly reduces the toxicity in ALS in a yeast model. Co-chaperone Hsc70 is found to reduce the toxic TDP-43 aggregation in sporadic ALS patients [44]. In yeast, this finding is also novel.

We also find that the CG32641 and CG6693 chaperones rescue the FUS toxicity in yeast cells, which is also not previously known.

The hypothetical model in **Fig.3** shows the mechanism of action

In this study, we have used a cloned library of 38 DnaJ domain chaperones of flies and expressed them in two ALS mutants, TDP-43 and FUS. This will help shed some light on the differences and similarities in the pathways regulated by TDP-43 and FUS in the pathogenesis of ALS.

465 **4.0 Material and Methods**

466 **4.1 Cloning of DNAJ domain chaperones and co-chaperones (Hsp40, Hsc70 and Hsp70)**
467 **library in yeast**

468 *Drosophila* Hsp40 and Hsp70 proteins were cloned by the Topo-D-Entr cloning kit (Invitrogen)
469 into the Topo-D-Entr vector. This was done post-PCR amplification using gene-specific
470 primers. Constructs were confirmed by sequencing and were transferred to the destination
471 vector pUASgHA for Hsp40 and pUASt-ccdB-FLAG (pTWF) for Hsp70.

472 For expression of Hsp40 and Hsp70 in yeast cells, Topo-D-Entr clones were cloned in the
473 destination vector pAG424GALccdB-HA with a 3X HA tag at the C-terminal [73]. The protein
474 expression of each isoform was confirmed by immunoblotting using either an anti-HA antibody
475 or an anti-FLAG antibody accordingly.

476

477 **4.2 Construction of yeast overexpression of DnaJ chaperones and co-chaperones in yeast**
478 **TDP-43 and FUS strains backgrounds:**

479 **4.2.1 Bacterial Transformation**

480 For the bacterial transformation, DH5αCells were made competent by using the calcium
481 chloride method. 200µl competent cells were taken, and 1 µl plasmid DNA of ALS plasmids
482 pRS426 Gal-TDP-43-GFP and pAG416 Gal-FUS-YFP were added. Incubated on ice for half
483 an hour. Then, heat shock was given for 2 minutes at 42°C, and it was kept on ice for 1 minute.
484 Then 900 µl Luria Broth was added to it, and it was incubated at 37°C for 30 to 45 minutes.
485 The cells were centrifuged at 8000 rpm for 3 minutes at room temperature. Then, the
486 supernatant was discarded, and the cells were resuspended in 200 µl of Luria broth.
487 They were plated with glass beads on LB amp plates, and finally, the plates were incubated
488 overnight (maximum 18 hours) at 37°C. These plasmids were deposited by Aron Gilter,
489 numbered 27467 and 29592, respectively.

4.2.2 Plasmid Isolation:

A single colony of transformed bacteria was inoculated in 5ml LB broth, and 5µl of Ampicillin was added and kept in a 37°C shaker overnight. The culture was centrifuged at 10,000 rpm for 5 minutes, and 100µl of GET was added. The culture was incubated on ice for 2 minutes. 200µl of alkaline SDS was added to it. Incubated on ice for 2 minutes, and 150µl of acidic KoAc was added and incubated again on ice for 5 minutes. The whole culture was centrifuged at 14,000 rpm for 5 minutes at 4°C. The supernatant was collected, and 400µl of phenol: chloroform solution was added. Centrifuged at 14,000 rpm for 5 minutes at 4°C. The aqueous phase was collected, and 1 mL of 100% ethanol was added. This was kept at -20°c for 15 minutes for precipitation and centrifuged at 14,000 rpm for 10 minutes at 4°C. The supernatant was decanted, and the pellet was washed with 500µl of 70% ethanol by centrifuging it at 14,000 rpm for 5 minutes at 4°C. Then, the supernatant was discarded, and the pellet was air-dried. Once it dried, the pellet was resuspended in 50µl of TE buffer. Finally, the plasmid was stored at 20°C.

4.2.3 Yeast Transformation:

Yeast strain *Saccharomyces cerevisiae* (w303a, MATa, ade2, his3, leu2, trp1, ura3) cells were grown in 5 ml YPD (yeast extract, peptone, and dextrose) medium, i.e., Primary culture, and allowed to grow overnight at 30°C, aerobically. Then, 15 ml YPD media was added to the primary culture to make a volume of 20 ml and allowed to grow for another 3-4 hours. After spinning down the cells at 5000 rpm for 5 minutes at room temperature, the pellet was resuspended in 1 ml autoclaved distilled water to wash off residual media and transferred to a 1.5 ml tube. The pellet was resuspended completely after spinning down in 500 µl LiOAc, from which 50 µl aliquots were made as per the number of transformations to be performed. Cells were centrifuged, and to each vial, 50% Polyethylene Glycol, 1 M Lithium acetate, 5µl ss DNA, and plasmid DNA were added [74]. The cell suspension was vortexed to ensure resuspension

and subjected to a heat shock at 42°C for 45 minutes in a water bath. The cell suspension was centrifuged at 5000 rpm for 5 min at room temperature, and 200 µl autoclaved distilled water was used to resuspend the pellet.

The plasmids TDP-43 and FUS are galactose inducible and have an Uracil marker and are placed on SD-Ura, having a mixture of Sucrose, YNB, and amino acid lacking mixture Uracil. The media used were from Clontech Laboratories. USA. The plates were incubated at 30°C for 3-4 days [75]

In the case of the DnaJ domain chaperone, double transformation was done with ALS mutants. These chaperones have a Trp marker. Transformation was done on SD-Trp-Ura (YNB, dextrose, agar, and amino acid mixture lacking Tryptophan and Uracil) medium.

4.3 Serial dilution assay:

A single colony was inoculated of the transformed cultures of TDP-43 and FUS in 500µl media of SD-Ura and allowed to grow overnight on a shaking incubator at 30°C. Raf-Ura (YNB, raffinose and amino acid mixture lacking Tryptophan and Uracil) washes were given, i.e., dextrose in the medium was replaced by raffinose, and their O.D was adjusted to 0.2 at 600 nm and allowed to grow again in the same conditions. Next day, the O.D was adjusted to 0.2, and the culture was diluted up to 1/10000th dilution (10^0 to 10^{-5}dilutions) and 3-6 µl of each dilution was spotted on approximate SD-Ura and SGal-Ura (galactose, YNB, Agar and amino acid mixture lacking Tryptophan and Uracil) plates and incubated at 30^0C for 2-4 days as all the plasmids used are galactose inducible.

For the double transformation of ALS mutant strains, two clones were selected and inoculated into an SD-Trp-Ura medium. Further plated on SD-Trp-Ura and SGal-Trp-Ura plates with control luciferase.

4.4 Growth Assay:

Transformed colonies of double transformants were inoculated in SD-Trp-Ura (Sucrose, YNB, and amino acid lacking mixture Uracil) medium overnight on a shaking incubator at 30°C. The next day, Raf-Trp-Ura (Raffinose, YNB, and amino acid lacking mixture Tryptophan Uracil) washes were given, and their O.D. was adjusted to 0.2 at 600nm on the same day 20% galactose was added to each culture in 540 µl Raf-Trp-Ura and the cultures were added in 96 well plates in triplicates with blank (Raf-Trp-Ura + Gal).96-well plate was placed in an Epoch2 BioTek Spectrophotometer for 48 hours at 30°C with continuous orbital shaking, and O.D. was measured every 30 min. The data obtained after 48 hrs were plotted in GraphPad software, and the Growth curve was plotted for each culture.

4.5 Microscopy:

By using fluorescence microscopy, we analysed the protein aggregation status of the yeast cells as the FUS and TDP43 constructs had a GFP tag.All transformed *S. cerevisiae* strains were grown overnight in an SD-Trp-Ura broth at 30°C. The next day, they were subjected to Raf-Trp-Ura$^-$ wash for the removal of residual dextrose. O.D was adjusted to 0.2 in Raf-Trp-Ura$^-$. After 2-3 hours, they were induced by 50 µl 20% galactose. Next day, they were centrifuged and resuspended in the residual media, and smear was prepared and observed under a confocal microscope under 60x objective and GFP laser. Images were processed using FIGI software.

4.5.1 Quantitation of Image Analysis:

Mutant strains transformed with different chaperones displaying two different morphology punctae and diffused cytoplasm. These were counted in 3 biological replicates for each strain. Chaperones that show more diffused cytoplasm and fewer punctae compared to luciferase are classified as suppressors, and chaperones that show higher punctae and less diffused cytoplasm compared to luciferase are classified as enhancers.

564 **5.0 References: -**

565 1. Ghasemi M, Brown RH. Genetics of Amyotrophic Lateral Sclerosis. Cold Spring Harb
566 Perspect Med. 2018;8. doi:10.1101/cshperspect.a024125

567 2. Rosen DR, Siddique T, Patterson D, Figlewicz DA, Sapp P, Hentati A, et al. Mutations
568 in Cu/Zn superoxide dismutase gene are associated with familial amyotrophic lateral
569 sclerosis. Nature. 1993;362: 59–62. doi:10.1038/362059a0

570 3. Johnson JO, Mandrioli J, Benatar M, Abramzon Y, Van Deerlin VM, Trojanowski JQ,
571 et al. Exome Sequencing Reveals VCP Mutations as a Cause of Familial ALS. Neuron.
572 2010;68: 857–864. doi:10.1016/j.neuron.2010.11.036

573 4. Cirulli ET, Lasseigne BN, Petrovski S, Sapp PC, Dion PA, Leblond CS, et al. Exome
574 sequencing in amyotrophic lateral sclerosis identifies risk genes and pathways. Science
575 (1979). 2015;347: 1436–1441. doi:10.1126/science.aaa3650

576 5. Armon C. Smoking may be considered an established risk factor for sporadic ALS.
577 Neurology. 2009;73: 1693–8. doi:10.1212/WNL.0b013e3181c1df48

578 6. de Jong SW, Huisman MHB, Sutedja NA, van der Kooi AJ, de Visser M, Schelhaas
579 HJ, et al. Smoking, alcohol consumption, and the risk of amyotrophic lateral sclerosis:
580 a population-based study. Am J Epidemiol. 2012;176: 233–9. doi:10.1093/aje/kws015

581 7. Lagier-Tourenne C, Cleveland DW. Rethinking ALS: the FUS about TDP-43. Cell.
582 2009;136: 1001–4. doi:10.1016/j.cell.2009.03.006

583 8. Gitler AD, Shorter J. RNA-binding proteins with prion-like domains in ALS and
584 FTLD-U. Prion. 2011;5: 179–187. doi:10.4161/pri.5.3.17230

585 9. Arai T, Hasegawa M, Akiyama H, Ikeda K, Nonaka T, Mori H, et al. TDP-43 is a
586 component of ubiquitin-positive tau-negative inclusions in frontotemporal lobar
587 degeneration and amyotrophic lateral sclerosis. Biochem Biophys Res Commun.
588 2006;351: 602–611. doi:10.1016/j.bbrc.2006.10.093

589 10. Neumann M, Sampathu DM, Kwong LK, Truax AC, Micsenyi MC, Chou TT, et al.
590 Ubiquitinated TDP-43 in Frontotemporal Lobar Degeneration and Amyotrophic
591 Lateral Sclerosis. Science (1979). 2006;314: 130–133. doi:10.1126/science.1134108

592 11. Vance C, Rogelj B, Hortobágyi T, De Vos KJ, Nishimura AL, Sreedharan J, et al.
593 Mutations in FUS, an RNA processing protein, cause familial amyotrophic lateral
594 sclerosis type 6. Science. 2009;323: 1208–1211. doi:10.1126/science.1165942

595 12. Kwiatkowski TJ, Bosco DA, LeClerc AL, Tamrazian E, Vanderburg CR, Russ C, et al.
596 Mutations in the *FUS/TLS* Gene on Chromosome 16 Cause Familial Amyotrophic
597 Lateral Sclerosis. Science (1979). 2009;323: 1205–1208. doi:10.1126/science.1166066

598 13. Sun Z, Diaz Z, Fang X, Hart MP, Chesi A, Shorter J, et al. Molecular determinants and
599 genetic modifiers of aggregation and toxicity for the ALS disease protein FUS/TLS.
600 PLoS Biol. 2011;9: e1000614. doi:10.1371/journal.pbio.1000614

601 14. Watanabe M, Dykes-Hoberg M, Cizewski Culotta V, Price DL, Wong PC, Rothstein
602 JD. Histological Evidence of Protein Aggregation in Mutant SOD1 Transgenic Mice

603 and in Amyotrophic Lateral Sclerosis Neural Tissues. Neurobiol Dis. 2001;8: 933–941.
604 doi:10.1006/nbdi.2001.0443

605 15. Mogk A, Bukau B. Protein quality control systems: Mechanisms and applications.
606 Microb Cell Fact. 2006;5: S8. doi:10.1186/1475-2859-5-S1-S8

607 16. Kampinga HH, Bergink S. Heat shock proteins as potential targets for protective
608 strategies in neurodegeneration. Lancet Neurol. 2016;15: 748–759.
609 doi:10.1016/S1474-4422(16)00099-5

610 17. Carrell RW, Lomas DA. Conformational disease. Lancet. 1997;350: 134–8.
611 doi:10.1016/S0140-6736(97)02073-4

612 18. Goedert M. Tau protein and neurodegeneration. Semin Cell Dev Biol. 2004;15: 45–49.
613 doi:10.1016/j.semcdb.2003.12.015

614 19. Martindale D, Hackam A, Wieczorek A, Ellerby L, Wellington C, McCutcheon K, et
615 al. Length of huntingtin and its polyglutamine tract influences localization and
616 frequency of intracellular aggregates. Nat Genet. 1998;18: 150–154.
617 doi:10.1038/ng0298-150

618 20. Johnson BS, McCaffery JM, Lindquist S, Gitler AD. A yeast TDP-43 proteinopathy
619 model: Exploring the molecular determinants of TDP-43 aggregation and cellular
620 toxicity. Proc Natl Acad Sci U S A. 2008;105: 6439–44. doi:10.1073/pnas.0802082105

621 21. Johnson BS, Snead D, Lee JJ, McCaffery JM, Shorter J, Gitler AD. TDP-43 Is
622 Intrinsically Aggregation-prone, and Amyotrophic Lateral Sclerosis-linked Mutations
623 Accelerate Aggregation and Increase Toxicity. Journal of Biological Chemistry.
624 2009;284: 20329–20339. doi:10.1074/jbc.M109.010264

625 22. Beissinger M, Buchner J. How chaperones fold proteins. Biol Chem. 1998;379: 245–
626 59.

627 23. Bar-Lavan Y, Shemesh N, Ben-Zvi A. Chaperone families and interactions in metazoa.
628 Essays Biochem. 2016;60: 237–253. doi:10.1042/EBC20160004

629 24. Bascos NAD, Landry SJ. A History of Molecular Chaperone Structures in the Protein
630 Data Bank. Int J Mol Sci. 2019;20. doi:10.3390/ijms20246195

631 25. Tsai J, Douglas MG. A Conserved HPD Sequence of the J-domain Is Necessary for
632 YDJ1 Stimulation of Hsp70 ATPase Activity at a Site Distinct from Substrate Binding.
633 Journal of Biological Chemistry. 1996;271: 9347–9354. doi:10.1074/jbc.271.16.9347

634 26. Cheetham ME, Caplan AJ. Structure, function and evolution of DnaJ: conservation and
635 adaptation of chaperone function. Cell Stress Chaperones. 1998;3: 28.
636 doi:10.1379/1466-1268(1998)003<0028:SFAEOD>2.3.CO;2

637 27. Caplan AJ. What is a co-chaperone? Cell Stress Chaperones. 2003;8: 105–7.
638 doi:10.1379/1466-1268(2003)008<0105:wiac>2.0.co;2

639 28. Morimoto RI, Santoro MG. Stress–inducible responses and heat shock proteins: New
640 pharmacologic targets for cytoprotection. Nat Biotechnol. 1998;16: 833–838.
641 doi:10.1038/nbt0998-833

642 29. Lindquist S. Regulation of protein synthesis during heat shock. Nature. 1981;293:
643 311–314. doi:10.1038/293311a0

644 30. Deo A, Ghosh R, Ahire S, Marathe S, Majumdar A, Bose T. Two novel DnaJ
645 chaperone proteins CG5001 and P58IPK regulate the pathogenicity of Huntington's
646 disease related aggregates. Sci Rep. 2024;14: 20867. doi:10.1038/s41598-024-71065-3

647 31. Desai M, Hemant, Deo A, Naik J, Dhamale P, Kshirsagar A, et al. Mrj is a chaperone
648 of the Hsp40 family that regulates Orb2 oligomerization and long-term memory in
649 Drosophila. PLoS Biol. 2024;22: e3002585. doi:10.1371/journal.pbio.3002585

650 32. Vance C, Rogelj B, Hortobágyi T, De Vos KJ, Nishimura AL, Sreedharan J, et al.
651 Mutations in FUS, an RNA Processing Protein, Cause Familial Amyotrophic Lateral
652 Sclerosis Type 6. Science (1979). 2009;323: 1208–1211. doi:10.1126/science.1165942

653 33. Park S-K, Hong JY, Arslan F, Kanneganti V, Patel B, Tietsort A, et al. Overexpression
654 of the essential Sis1 chaperone reduces TDP-43 effects on toxicity and proteolysis.
655 PLoS Genet. 2017;13: e1006805. doi:10.1371/journal.pgen.1006805

656 34. Gu J, Wang C, Hu R, Li Y, Zhang S, Sun Y, et al. Hsp70 chaperones TDP-43 in
657 dynamic, liquid-like phase and prevents it from amyloid aggregation. Cell Res.
658 2021;31: 1024–1027. doi:10.1038/s41422-021-00526-5

659 35. Molliex A, Temirov J, Lee J, Coughlin M, Kanagaraj AP, Kim HJ, et al. Phase
660 Separation by Low Complexity Domains Promotes Stress Granule Assembly and
661 Drives Pathological Fibrillization. Cell. 2015;163: 123–133.
662 doi:10.1016/j.cell.2015.09.015

663 36. Li H-R, Chiang W-C, Chou P-C, Wang W-J, Huang J. TAR DNA-binding protein 43
664 (TDP-43) liquid–liquid phase separation is mediated by just a few aromatic residues.
665 Journal of Biological Chemistry. 2018;293: 6090–6098.
666 doi:10.1074/jbc.AC117.001037

667 37. Liu Z, Zhang S, Gu J, Tong Y, Li Y, Gui X, et al. Hsp27 chaperones FUS phase
668 separation under the modulation of stress-induced phosphorylation. Nat Struct Mol
669 Biol. 2020;27: 363–372. doi:10.1038/s41594-020-0399-3

670 38. Gaudet P, Livstone MS, Lewis SE, Thomas PD. Phylogenetic-based propagation of
671 functional annotations within the Gene Ontology consortium. Brief Bioinform.
672 2011;12: 449–462. doi:10.1093/bib/bbr042

673 39. R. RK, N. S. N, S. P. A, Sinha D, Veedin Rajan VB, Esthaki VK, et al. HSPIR: a
674 manually annotated heat shock protein information resource. Bioinformatics. 2012;28:
675 2853–2855. doi:10.1093/bioinformatics/bts520

676 40. LIU T, JIANG W, HAN D, YU L. DNAJC25 is downregulated in hepatocellular
677 carcinoma and is a novel tumor suppressor gene. Oncol Lett. 2012;4: 1274–1280.
678 doi:10.3892/ol.2012.903

679 41. Yabe I, Tanino M, Yaguchi H, Takiyama A, Cai H, Kanno H, et al. Pathology of
680 frontotemporal dementia with limb girdle muscular dystrophy caused by a DNAJB6

mutation. Clin Neurol Neurosurg. 2014;127: 10–12. doi:10.1016/j.clineuro.2014.09.013

42. Kakkar V, Månsson C, de Mattos EP, Bergink S, van der Zwaag M, van Waarde MAWH, et al. The S/T-Rich Motif in the DNAJB6 Chaperone Delays Polyglutamine Aggregation and the Onset of Disease in a Mouse Model. Mol Cell. 2016;62: 272–283. doi:10.1016/j.molcel.2016.03.017

43. Aprile FA, Källstig E, Limorenko G, Vendruscolo M, Ron D, Hansen C. The molecular chaperones DNAJB6 and Hsp70 cooperate to suppress α-synuclein aggregation. Sci Rep. 2017;7: 9039. doi:10.1038/s41598-017-08324-z

44. Arosio A, Cristofani R, Pansarasa O, Crippa V, Riva C, Sirtori R, et al. HSC70 expression is reduced in lymphomonocytes of sporadic ALS patients and contributes to TDP-43 accumulation. Amyotroph Lateral Scler Frontotemporal Degener. 2020;21: 51–62. doi:10.1080/21678421.2019.1672749

45. Richter K, Haslbeck M, Buchner J. The heat shock response: life on the verge of death. Mol Cell. 2010;40: 253–66. doi:10.1016/j.molcel.2010.10.006

46. Liu T, Daniels CK, Cao S. Comprehensive review on the HSC70 functions, interactions with related molecules and involvement in clinical diseases and therapeutic potential. Pharmacol Ther. 2012;136: 354–374. doi:10.1016/j.pharmthera.2012.08.014

47. Stricher F, Macri C, Ruff M, Muller S. HSPA8/HSC70 chaperone protein. Autophagy. 2013;9: 1937–1954. doi:10.4161/auto.26448

48. Zhang Z, Jing J, Ye Y, Chen Z, Jing Y, Li S, et al. Characterization of the dual functional effects of heat shock proteins (HSPs) in cancer hallmarks to aid development of HSP inhibitors. Genome Med. 2020;12: 101. doi:10.1186/s13073-020-00795-6

49. Hammond CM, Bao H, Hendriks IA, Carraro M, García-Nieto A, Liu Y, et al. DNAJC9 integrates heat shock molecular chaperones into the histone chaperone network. Mol Cell. 2021;81: 2533-2548.e9. doi:10.1016/j.molcel.2021.03.041

50. Lai CW, Otero JH, Hendershot LM, Snapp E. ERdj4 Protein Is a Soluble Endoplasmic Reticulum (ER) DnaJ Family Protein That Interacts with ER-associated Degradation Machinery. Journal of Biological Chemistry. 2012;287: 7969–7978. doi:10.1074/jbc.M111.311290

51. Huang Y, Arora K, Mun KS, Yang F, Moon C, Yarlagadda S, et al. Targeting DNAJB9, a novel ER luminal co-chaperone, to rescue ΔF508-CFTR. Sci Rep. 2019;9: 9808. doi:10.1038/s41598-019-46161-4

52. Liu D, Zuo R, Liu W, He Y, Wang Y, Yue P, et al. <scp>DNAJC24</scp> acts directly with <scp>PCNA</scp> and promotes malignant progression of <scp>LUAD</scp> by activating phosphorylation of <scp>AKT</scp>. The FASEB Journal. 2024;38. doi:10.1096/fj.202300667RR

720 53. Veenma D, Cordeiro D, Sondheimer N, Mercimek-Andrews S. DNAJC12-associated
721 developmental delay, movement disorder, and mild hyperphenylalaninemia identified
722 by whole-exome sequencing re-analysis. European Journal of Human Genetics.
723 2018;26: 1867–1870. doi:10.1038/s41431-018-0237-9

724 54. Uhrigshardt H, Rouault TA, Missirlis F. Insertion mutants in Drosophila melanogaster
725 Hsc20 halt larval growth and lead to reduced iron–sulfur cluster enzyme activities and
726 impaired iron homeostasis. JBIC Journal of Biological Inorganic Chemistry. 2013;18:
727 441–449. doi:10.1007/s00775-013-0988-2

728 55. Thomson DW, Dinger ME. Endogenous microRNA sponges: evidence and
729 controversy. Nat Rev Genet. 2016;17: 272–283. doi:10.1038/nrg.2016.20

730 56. Johnson BS, McCaffery JM, Lindquist S, Gitler AD. A yeast TDP-43 proteinopathy
731 model: Exploring the molecular determinants of TDP-43 aggregation and cellular
732 toxicity. Proceedings of the National Academy of Sciences. 2008;105: 6439–6444.
733 doi:10.1073/pnas.0802082105

734 57. Tomoyasu T, Mogk A, Langen H, Goloubinoff P, Bukau B. Genetic dissection of the
735 roles of chaperones and proteases in protein folding and degradation in the *Escherichia*
736 *coli* cytosol. Mol Microbiol. 2001;40: 397–413. doi:10.1046/j.1365-
737 2958.2001.02383.x

738 58. Mogk A. Identification of thermolabile Escherichia coli proteins: prevention and
739 reversion of aggregation by DnaK and ClpB. EMBO J. 1999;18: 6934–6949.
740 doi:10.1093/emboj/18.24.6934

741 59. Lagier-Tourenne C, Polymenidou M, Cleveland DW. TDP-43 and FUS/TLS: emerging
742 roles in RNA processing and neurodegeneration. Hum Mol Genet. 2010;19: R46–R64.
743 doi:10.1093/hmg/ddq137

744 60. Kwiatkowski TJ, Bosco DA, LeClerc AL, Tamrazian E, Vanderburg CR, Russ C, et al.
745 Mutations in the *FUS/TLS* Gene on Chromosome 16 Cause Familial Amyotrophic
746 Lateral Sclerosis. Science (1979). 2009;323: 1205–1208. doi:10.1126/science.1166066

747 61. Gitler AD, Shorter J. RNA-binding proteins with prion-like domains in ALS and
748 FTLD-U. Prion. 2011;5: 179–187. doi:10.4161/pri.5.3.17230

749 62. Gitler AD. Beer and Bread to Brains and Beyond: Can Yeast Cells Teach Us about
750 Neurodegenerative Disease? Neurosignals. 2008;16: 52–62. doi:10.1159/000109759

751 63. Ju S, Tardiff DF, Han H, Divya K, Zhong Q, Maquat LE, et al. A Yeast Model of
752 FUS/TLS-Dependent Cytotoxicity. PLoS Biol. 2011;9: e1001052.
753 doi:10.1371/journal.pbio.1001052

754 64. Elden AC, Kim H-J, Hart MP, Chen-Plotkin AS, Johnson BS, Fang X, et al. Ataxin-2
755 intermediate-length polyglutamine expansions are associated with increased risk for
756 ALS. Nature. 2010;466: 1069–1075. doi:10.1038/nature09320

757 65. Lorenzetti D, Bohlega S, Zoghbi HY. The expansion of the CAG repeat in ataxin-2 is a
758 frequent cause of autosomal dominant spinocerebellar ataxia. Neurology. 1997;49:
759 1009–1013. doi:10.1212/WNL.49.4.1009

66. Barbieri EM, Linsenmeier M, Whiteman KR, Cheng Y, Braganza S, Copley KE, et al. Scouring the human Hsp70 network uncovers diverse chaperone safeguards buffering TDP-43 toxicity. 2025. doi:10.1101/2025.05.10.653282

67. LIU T, JIANG W, HAN D, YU L. DNAJC25 is downregulated in hepatocellular carcinoma and is a novel tumor suppressor gene. Oncol Lett. 2012;4: 1274–1280. doi:10.3892/ol.2012.903

68. Braell WA, Schlossman DM, Schmid SL, Rothman JE. Dissociation of clathrin coats coupled to the hydrolysis of ATP: role of an uncoating ATPase. J Cell Biol. 1984;99: 734–741. doi:10.1083/jcb.99.2.734

69. Wu E, He W, Wu C, Chen Z, Zhou S, Wu X, et al. HSPA8 acts as an amyloidase to suppress necroptosis by inhibiting and reversing functional amyloid formation. Cell Res. 2023;33: 851–866. doi:10.1038/s41422-023-00859-3

70. Incekara O, Acun T. DNAJC9 expression in basal-like and luminal A breast cancer subtypes predicts worse survival. Mol Biol Rep. 2023;50: 7275–7282. doi:10.1007/s11033-023-08654-4

71. Mandriani B, Castellana S, Rinaldi C, Manzoni M, Venuto S, Rodriguez-Aznar E, et al. Identification of p53-target genes in Danio rerio. Sci Rep. 2016;6: 32474. doi:10.1038/srep32474

72. Tummala H, Walne AJ, Williams M, Bockett N, Collopy L, Cardoso S, et al. DNAJC21 Mutations Link a Cancer-Prone Bone Marrow Failure Syndrome to Corruption in 60S Ribosome Subunit Maturation. Am J Hum Genet. 2016;99: 115–24. doi:10.1016/j.ajhg.2016.05.002

73. Hageman J, van Waarde MAWH, Zylicz A, Walerych D, Kampinga HH. The diverse members of the mammalian HSP70 machine show distinct chaperone-like activities. Biochemical Journal. 2011;435: 127–142. doi:10.1042/BJ20101247

74. Ito H, Fukuda Y, Murata K, Kimura A. Transformation of intact yeast cells treated with alkali cations. J Bacteriol. 1983;153: 163–168. doi:10.1128/jb.153.1.163-168.1983

75. Gietz RD, Schiestl RH. High-efficiency yeast transformation using the LiAc/SS carrier DNA/PEG method. Nat Protoc. 2007;2: 31–34. doi:10.1038/nprot.2007.13

6.0 Acknowledgment

This work was supported by a research grant from the Department of Biotechnology (DBT-IYBA) (BT/09/IYBA/2015/03), (DBT RLS) (BT/RLF/Re-entry/54/2013) to TB. SA recipients of the Indian Council of Medical Research (ICMR) senior research fellowship (SRF) (5/3/8/89/ITR-F/2020-ITR).

7.0 Declaration of interest

Conflict of interest: The authors declare no conflict of interest.

8.0 Figure Legends

Fig.1 Effect of DnaJ domain chaperones on the growth of ALS mutant TDP-43:

a. DnaJ domain chaperones transformed with ALS mutant TDP-43 were serially diluted and spotted on SD-Trp-Ura and SGal-Trp-Ura plates. In this figure, SGal-Trp-Ura was shown as a test with TDP-43, and luciferase was used as a control.

b. 48hrs growth curve of DnaJ domain chaperone transformed with TDP-43 mutant. Three biological replicate data were collected (n=3, $P<0.001$, paired t-test). The blue line indicates mutant TDP-43 with control luciferase, and the red line indicates DnaJ domain chaperones with the TDP-43 mutant.

c. Enhancers and suppressors of TDP-43 mutant based on the area under the curve values of the growth curve obtained using GraphPad Prism software. The area under the growth curve values is converted into the logarithmic scale and normalized. Chaperones on the right-hand side are the suppressors, and those on the left-hand side are enhancers.

Fig.1 Effect of DnaJ domain chaperones on the protein aggregation phenotype of the TDP-43 mutant of ALS

d. Microscopic images showing protein aggregation and diffused cytoplasm phenotype in the *Saccharomyces cerevisiae* model of ALS. Protein aggregation is seen in the form of bright GFP punctae in the cytoplasm after inducing with 20% Galactose.

e. Two different morphologies exhibited by the transformed DnaJ domain chaperones with the TDP-43 mutant. 100-150 cells were counted for each chaperone. The average score was plotted using GraphPad prism.

Fig.2 Effect of growth on ALS mutant due to chaperones (Spot dilution assay on Galactose medium)

826 **a**. Spot dilution assay on SGal-Trp-Ura medium of remaining DnaJ chaperones and
827 cochaperones mentioned in the study.

828 **b. Effect of chaperones on the growth of ALS mutant TDP-43 (48-hour growth curve)**

829 48-hr growth curve of the remaining 19 DnaJ domain chaperones with Luciferase as control.
830 Data shown in **Figure 2b** were obtained from three independent biological replicates (n=3,
831 P<0.05, paired t-test)
832 **c.** Enhancer and suppressor classification of the remaining 19 DnaJ domain chaperones with
833 TDP-43 mutant based on area under the curve values obtained from GraphPad prism. The
834 area under the curve values of each chaperone were converted to a logarithmic scale and
835 normalised. Plotted on GraphPad prism and obtained area under the curve graph on the right-
836 hand side are the suppressors, and the left-hand side are the enhancers.
837 **d. Effect of chaperones on the protein aggregation phenotype of TDP-43 mutant.**

838 19 different DnaJ chaperones and cochaperones showing protein aggregation in the
839 cytoplasm in the yeast model of ALS. After 20% galactose induction, microscopic images
840 were taken for each chaperone's protein aggregation was seen in the form of bright GFP
841 punctae.
842 **e.** Graph of 19 chaperones plotted in Graphpad prism shown in Figure **2c**. For each
843 chaperone, 100-150 cells were counted, and the average was plotted.

844 **Fig. 1 Effect of DnaJ domain chaperones on the growth of ALS mutant:**

845 **f.** DnaJ domain chaperones transformed with ALS mutant FUS were serially diluted and
846 spotted on SD-Trp-Ura and SGal-Trp-Ura plates. In this figure, SGal-Trp-Ura was shown as
847 a test with FUS luciferase as a control

848 **g**. 48-hour growth curve of DnaJ domain chaperone transformed with FUS mutant. Three
849 biological replicate data were collected (n=3, P<0.001, paired t-test). The blue line indicates
850 mutant FUS with control luciferase, and the red line indicates DNAJ domain chaperones with
851 the FUS mutant.

852 **h**.Enhancers and suppressors of TDP-43 mutant based on the area under the curve values of
853 the growth curve obtained using GraphPad prism software. The area under the growth curve

854 values is converted into the logarithmic scale and normalized. Chaperones on the right-hand
855 side are the suppressors, and on the left-hand side, chaperones are enhancers

856 **Fig.1 Effect of DnaJ domain chaperones on protein aggregation of FUS mutant**

857 **i.** Microscopic images showing protein aggregation and diffused cytoplasm phenotype in the
858 *Saccharomyces cerevisiae* model of ALS. Protein aggregation is seen in the form of bright
859 GFP punctae in the cytoplasm after inducing 20% Galactose.

860 **j**.Two different morphologies exhibited by the transformed DnaJ domain chaperones with the
861 FUS mutant. Counted 100-150 cells for each chaperone average was plotted on GraphPad
862 prism.

863 **Fig.2 Effect of growth on ALS mutant FUS due to chaperones (Spot dilution assay on**
864 **Galactose medium)**

865 **f**. Spot dilution assay on SGal-Trp-Ura medium of DnaJ chaperones and cochaperones with
866 the FUS mutant mentioned in this study shows a weak enhancer, and some show no effect.

867 **g.** 48-hour growth curve of DnaJ domain chaperone transformed with FUS mutant. Three
868 biological replicate data were collected (n=3, $P<0.001$, paired t-test). The blue line indicates
869 mutant FUS with control Luciferase, and the red line indicates DnaJ domain chaperones with
870 the FUS mutant described as a weak enhancer **a**nd some show no effect on the mutant FUS

871 **h**. Enhancer and suppressor classification of the remaining 21 DnaJ domain chaperones with
872 FUS mutant, based on the Area under the curve values obtained from GraphPad prism. The
873 area under the curve values of each chaperone were converted to a logarithmic scale and
874 normalized. Plotted on GraphPad prism and obtained Area Under the curve graph on the
875 right-hand side are the suppressors and on the left-hand side are the enhancers.
876

877 **Fig 2. Effect of DNAJ domain chaperones on the protein aggregation phenotype of the**
878 **FUS mutant of ALS.**

879 **f.** Different HSP40 chaperones and cochaperones are showing protein aggregation in the
880 cytoplasm in the yeast model of ALS. After 20% galactose induction for 24 hrs microscopic
881 images were taken for each chaperone's protein aggregation was seen in the form of bright
882 GFP punctae, indicating the weak enhancer. Some chaperones show both diffused cytoplasm
883 and protein aggregation phenotype as per the growth assay, and microscopic analysis
884 indicates they are either enhancers or suppressors and do not show a strong effect on the
885 mutant FUS.

886 **g**. Graph of 21 chaperones plotted in Graphpad prism is shown in Figure 2j. For each
887 chaperone counted 100-150 cells and the average was plotted.

888

889 **Fig.3 Hypothetical model**
890 This schematic diagram is the overall hypothesis of our research, in which the ALS mutant
891 genes of TDP-43 and FUS, when mutated, form misfolded proteins, resulting in an
892 aggregation of protein within the cell. by interacting with Hsp40 chaperones, i.e, Drosophila
893 DnaJ domain chaperones with yeast cells, they either enhance the toxicity or rescue the
894 toxicity of these two mutants. Toxic phenotype in yeast represents puncta in the cytoplasm,
895 and resue represents cytoplasmic diffusion.

896

897 **Supplementary Fig S1. TDP-43 and FUS plasmid.**
898 ALS plasmid TDP-43 and FUS sequence map.

899

900 **Supplementary Fig S2. ALS mutants TDP-43 and FUS and their effect on toxicity in**
901 **yeast cells.**

902 **S2a.** Spot dilution of plasmids TDP-43 and FUS with control after transformation in yeast.

903 **S2b.** 48hrs growth curve of TDP-43 and FUS, obtaining O.D. after 30 min at 600 nm (n=3,
904 P<0.05, paired t-test).

905 **S2b.** Confocal Microscopy of GFP-tagged plasmids TDP-43 and FUS with control.

906

907 **Supplementary Fig S3. DnaJ domain chaperones overexpression library construction.**

908 DnaJ domain chaperones overexpression library was created from flies, which are
909 homologous to the DnaJ domain proteins of humans, by Gateway cloning.

910

911 **Supplementary Fig S4. Effect of mutant TDP-43 and DnaJ chaperones on growth**

912 **S4a.** Enhancers and suppressors of TDP-43 are characterized based on the spot dilution assay
913 on the control plate SD-Trp-Ura.

914 **S4b.** Weak enhancer and suppressor classification based on spot dilution assay of TDP-43
915 chaperones on control SD-Trp-Ura.

916

917 **Supplementary Fig S5. Effect of mutant FUS and DnaJ chaperones on growth**

918 **S4a.**Enhancers and suppressors of FUS are characterized based on the spot dilution assay on
919 the control plate SD-Trp-Ura.

920 **S4b.**Weak enhancer and suppressor classification of FUS chaperones on control SD-Trp-Ura.

921

922 **Supplementary Fig S6. Phylogenetic tree for Hsp40 chaperones**

923 A phylogenetic tree was created using the Mega12 tool by using multiple sequence alignment
924 of the protein of chaperones across species.

925

926

927

928

929

930

931

Fig1 a

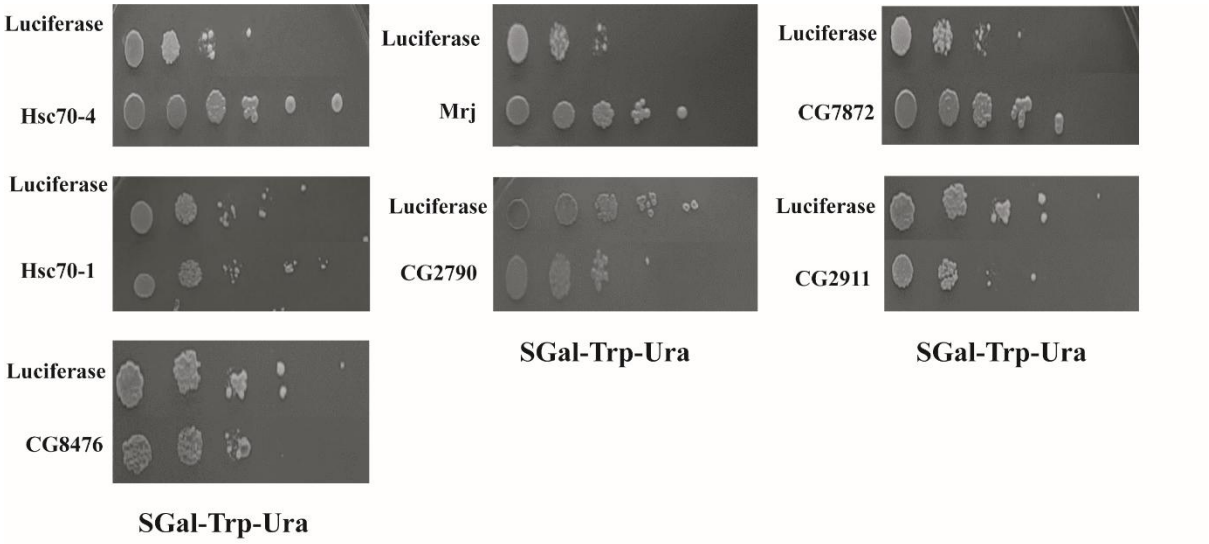
Luciferase
Hsc70-4
Luciferase
Mrj
Luciferase
CG7872
Luciferase
Hsc70-1
Luciferase
CG2790
Luciferase
CG2911
Luciferase
CG8476
SGal-Trp-Ura
SGal-Trp-Ura
SGal-Trp-Ura

1b

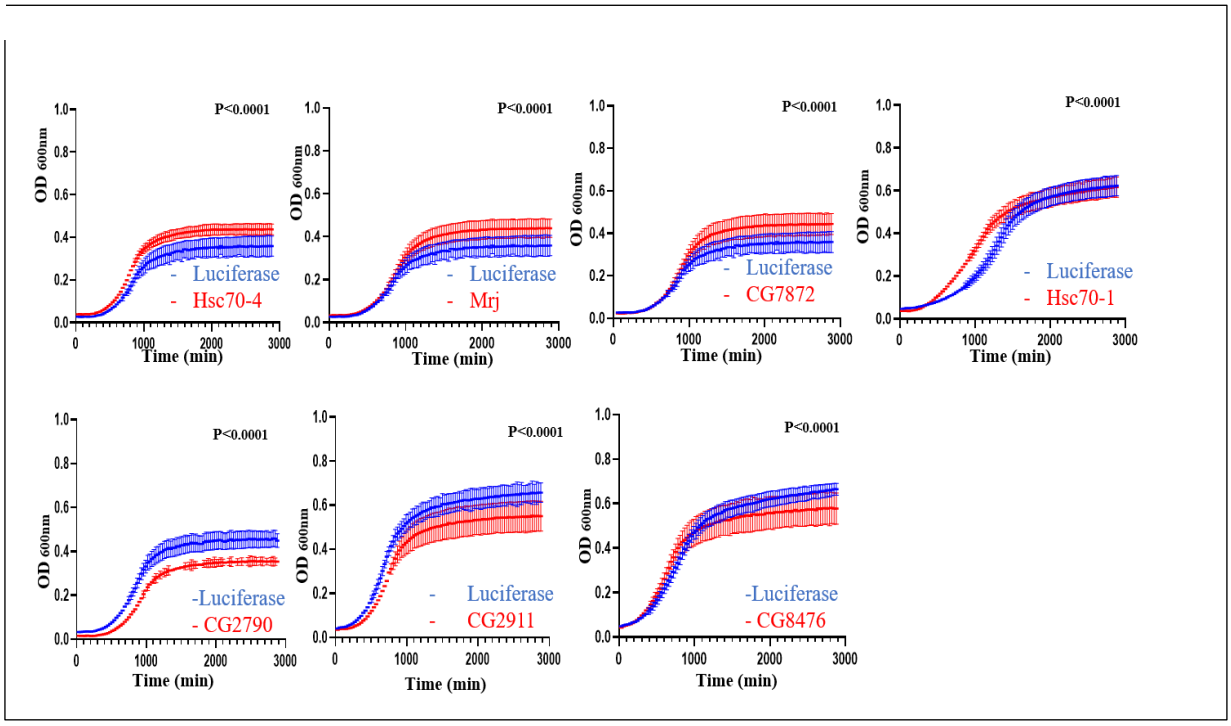
P<0.0001
OD 600nm
Time (min)
- Luciferase
- Hsc70-4
- Luciferase
- Mrj
- Luciferase
- CG7872
- Luciferase
- Hsc70-1
-Luciferase
- CG2790
- Luciferase
- CG2911
-Luciferase
- CG8476

1c

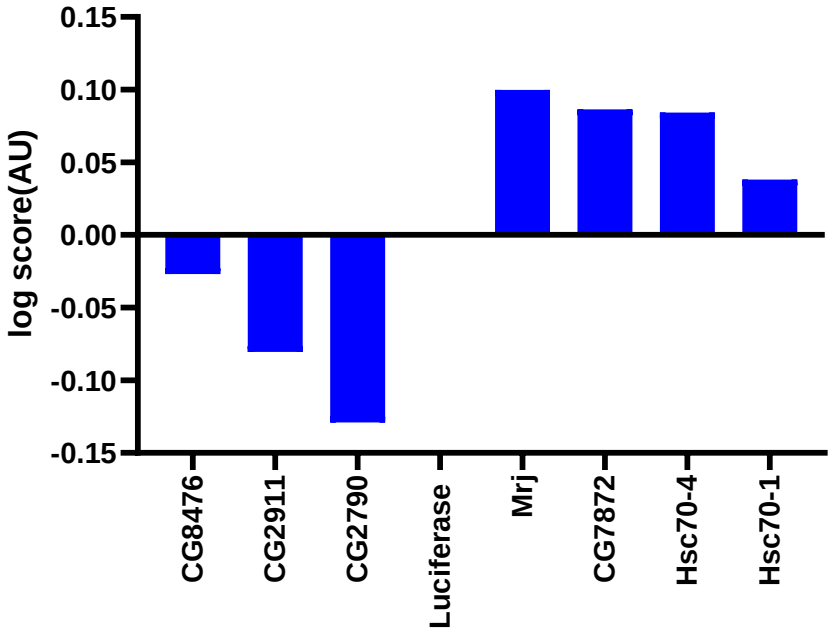
0.15
0.10
0.05
0.00
-0.05
-0.10
-0.15
log score(AU)
CG8476
CG2911
CG2790
Luciferase
Mrj
CG7872
Hsc70-4
Hsc70-1

1d

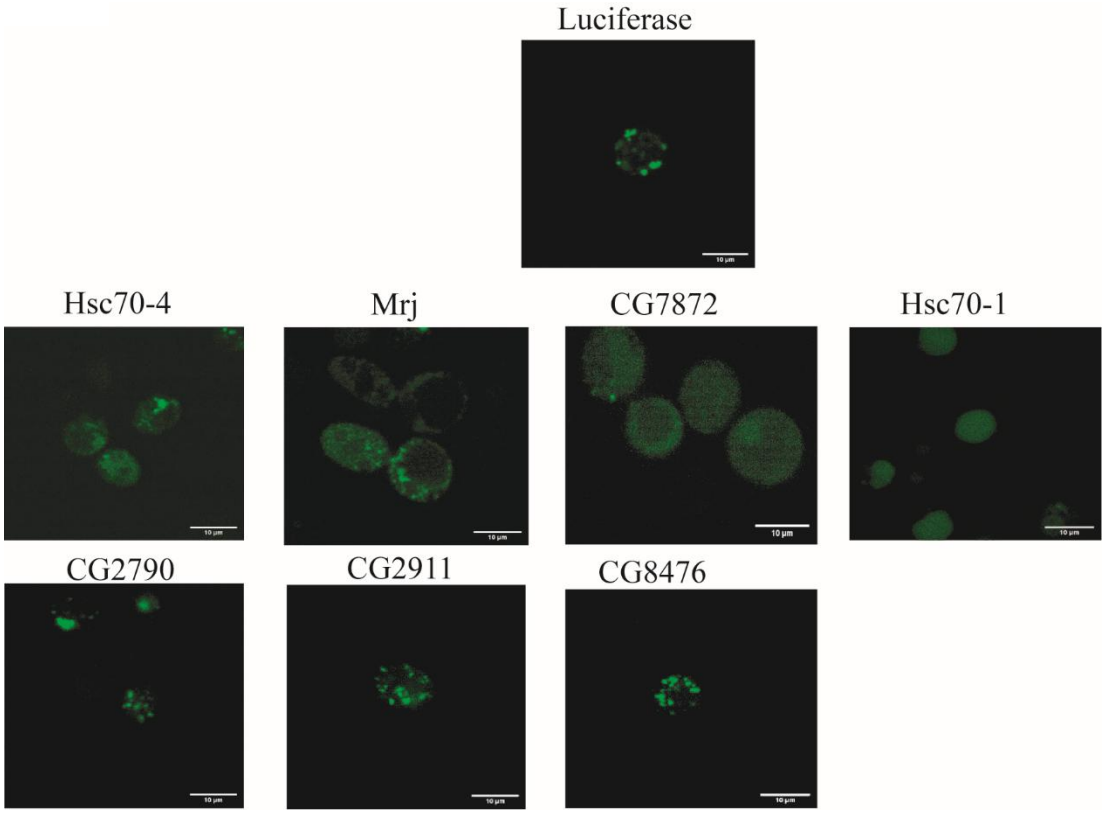
Luciferase
Hsc70-4
Mrj
CG7872
Hsc70-1
CG2790
CG2911
CG8476

1e

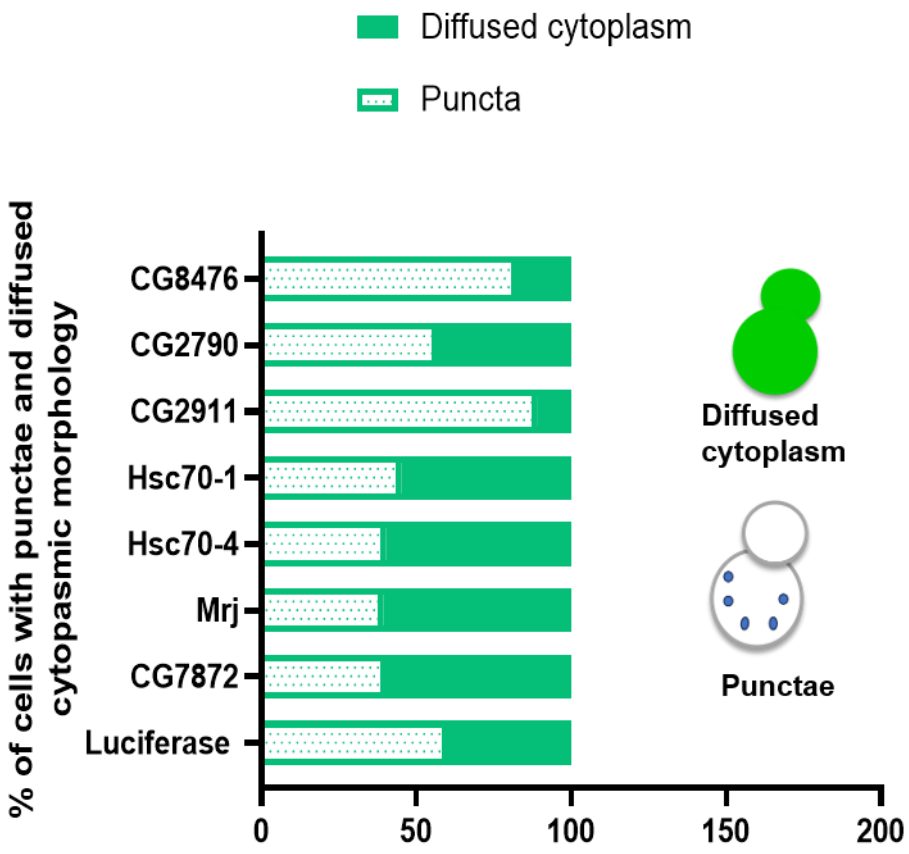
Diffused cytoplasm
Puncta
% of cells with punctae and diffused cytopasmic morphology
CG8476
CG2790
CG2911
Hsc70-1
Hsc70-4
Mrj
CG7872
Luciferase
0
50
100
150
200
Diffused cytoplasm
Punctae

Fig2 a

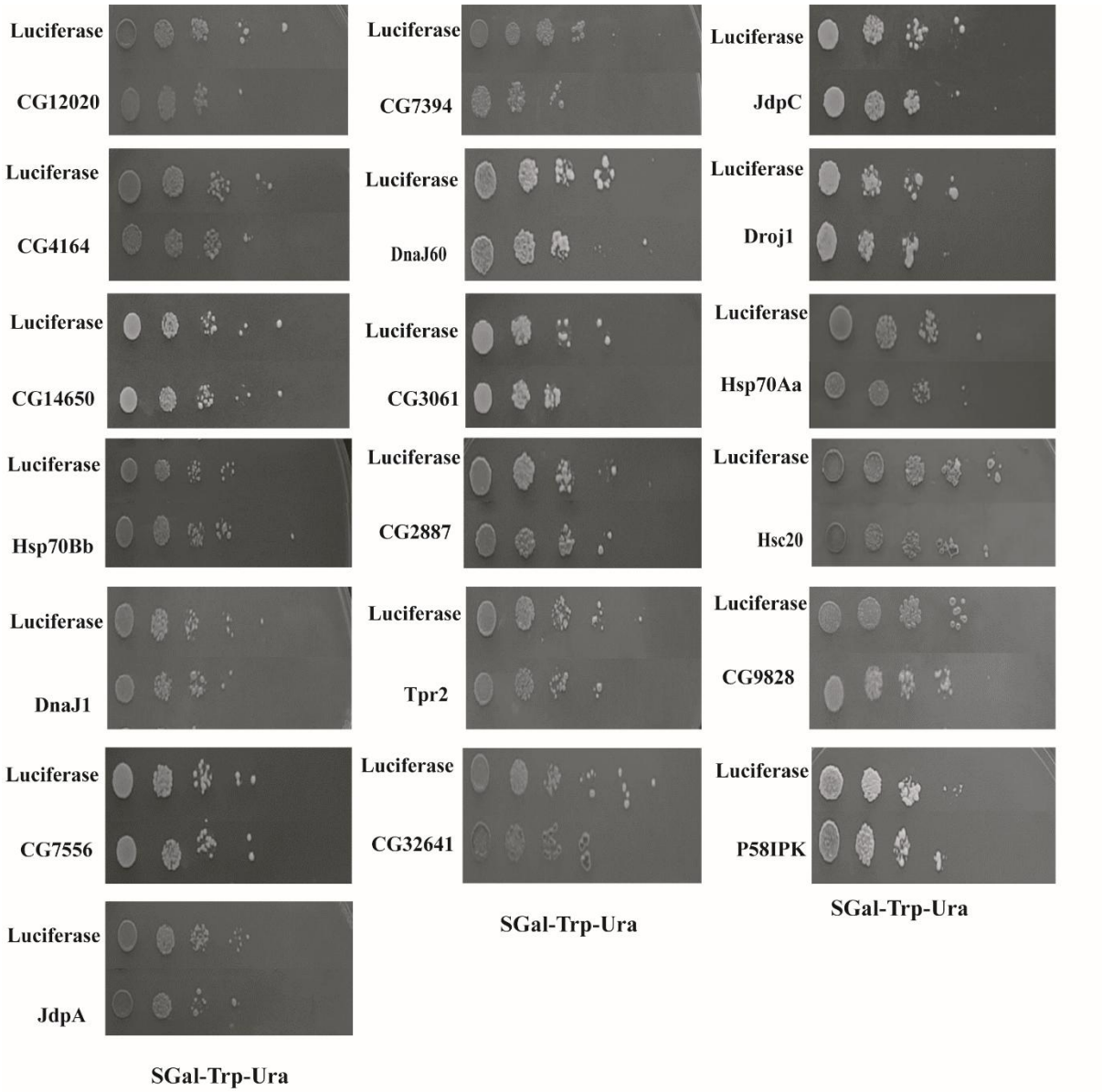
Luciferase
CG12020
Luciferase
CG4164
Luciferase
CG14650
Luciferase
Hsp70Bb
Luciferase
DnaJ1
Luciferase
CG7556
Luciferase
JdpA
SGal-Trp-Ura
Luciferase
CG7394
Luciferase
DnaJ60
Luciferase
CG3061
Luciferase
CG2887
Luciferase
Tpr2
Luciferase
CG32641
SGal-Trp-Ura
Luciferase
JdpC
Luciferase
Droj1
Luciferase
Hsp70Aa
Luciferase
Hsc20
Luciferase
CG9828
Luciferase
P58IPK
SGal-Trp-Ura

2b

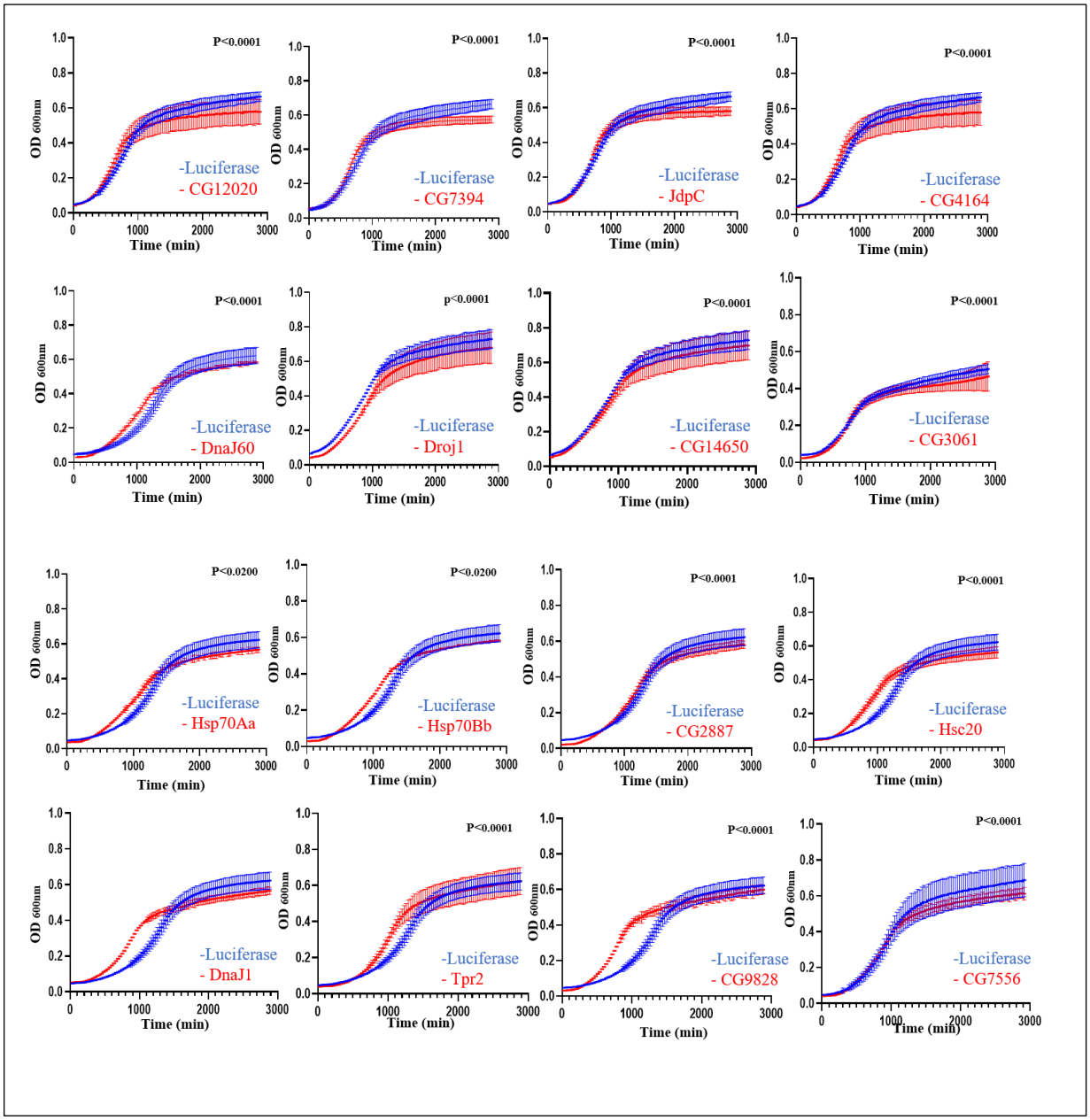
P<0.0001
-Luciferase
- CG12020
P<0.0001
-Luciferase
- CG7394
P<0.0001
-Luciferase
- JdpC
P<0.0001
-Luciferase
- CG4164
P<0.0001
-Luciferase
- DnaJ60
p<0.0001
-Luciferase
- Droj1
P<0.0001
-Luciferase
- CG14650
P<0.0001
-Luciferase
- CG3061
P<0.0200
-Luciferase
- Hsp70Aa
P<0.0200
-Luciferase
- Hsp70Bb
P<0.0001
-Luciferase
- CG2887
P<0.0001
-Luciferase
- Hsc20
-Luciferase
- DnaJ1
P<0.0001
-Luciferase
- Tpr2
P<0.0001
-Luciferase
- CG9828
P<0.0001
-Luciferase
- CG7556
OD 600nm
Time (min)

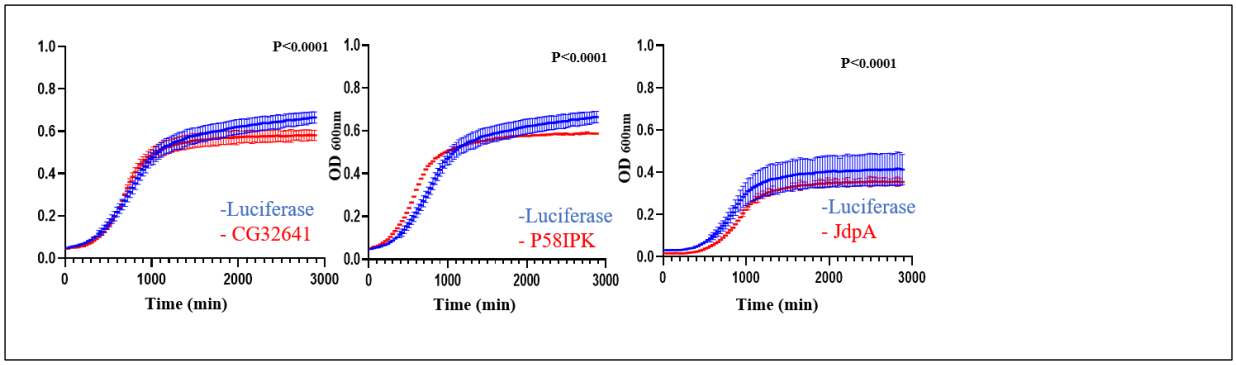
P<0.0001
-Luciferase
- CG32641
P<0.0001
-Luciferase
- P58IPK
P<0.0001
-Luciferase
- JdpA
OD 600nm
Time (min)

2c

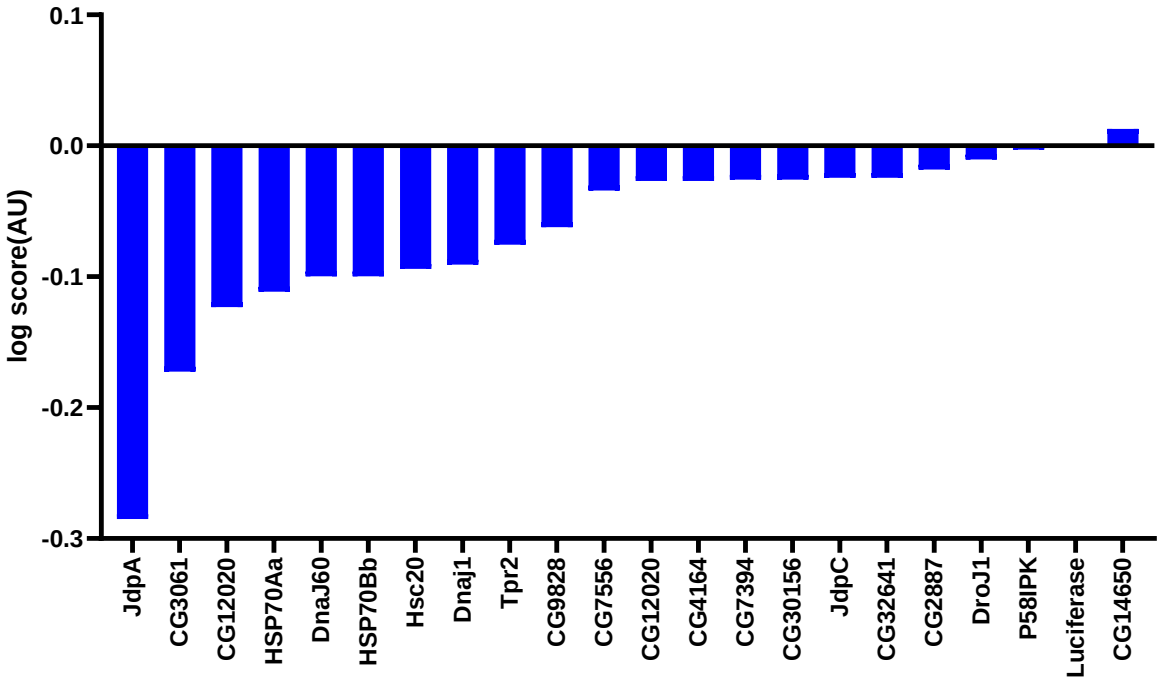
0.1
0.0
-0.1
-0.2
-0.3
log score(AU)
JdpA
CG3061
CG12020
HSP70Aa
DnaJ60
HSP70Bb
Hsc20
Dnaj1
Tpr2
CG9828
CG7556
CG12020
CG4164
CG7394
CG30156
JdpC
CG32641
CG2887
DroJ1
P58IPK
Luciferase
CG14650

2d

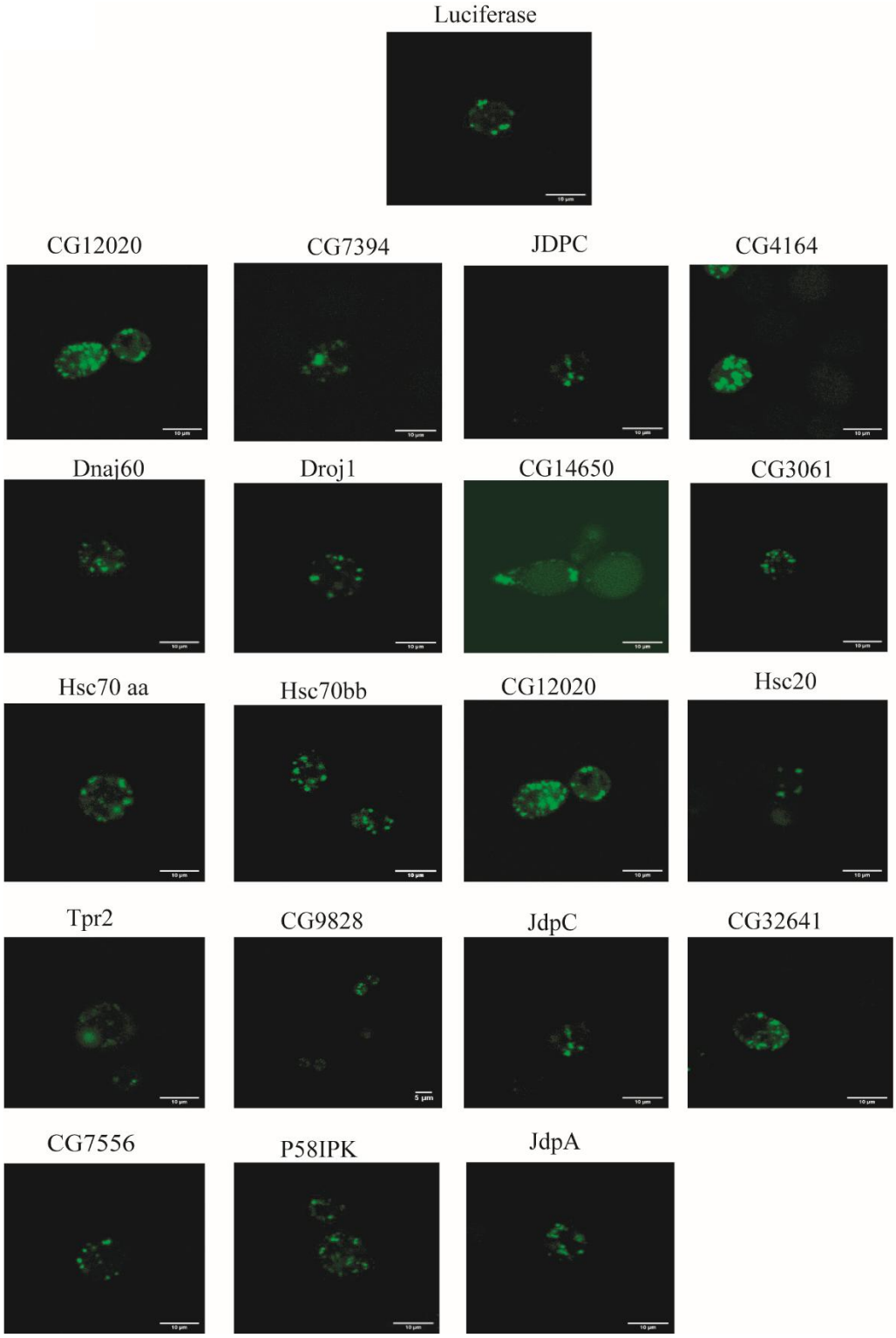
Luciferase
CG12020
CG7394
JDPC
CG4164
Dnaj60
Droj1
CG14650
CG3061
Hsc70 aa
Hsc70bb
CG12020
Hsc20
Tpr2
CG9828
JdpC
CG32641
CG7556
P58IPK
JdpA

2e

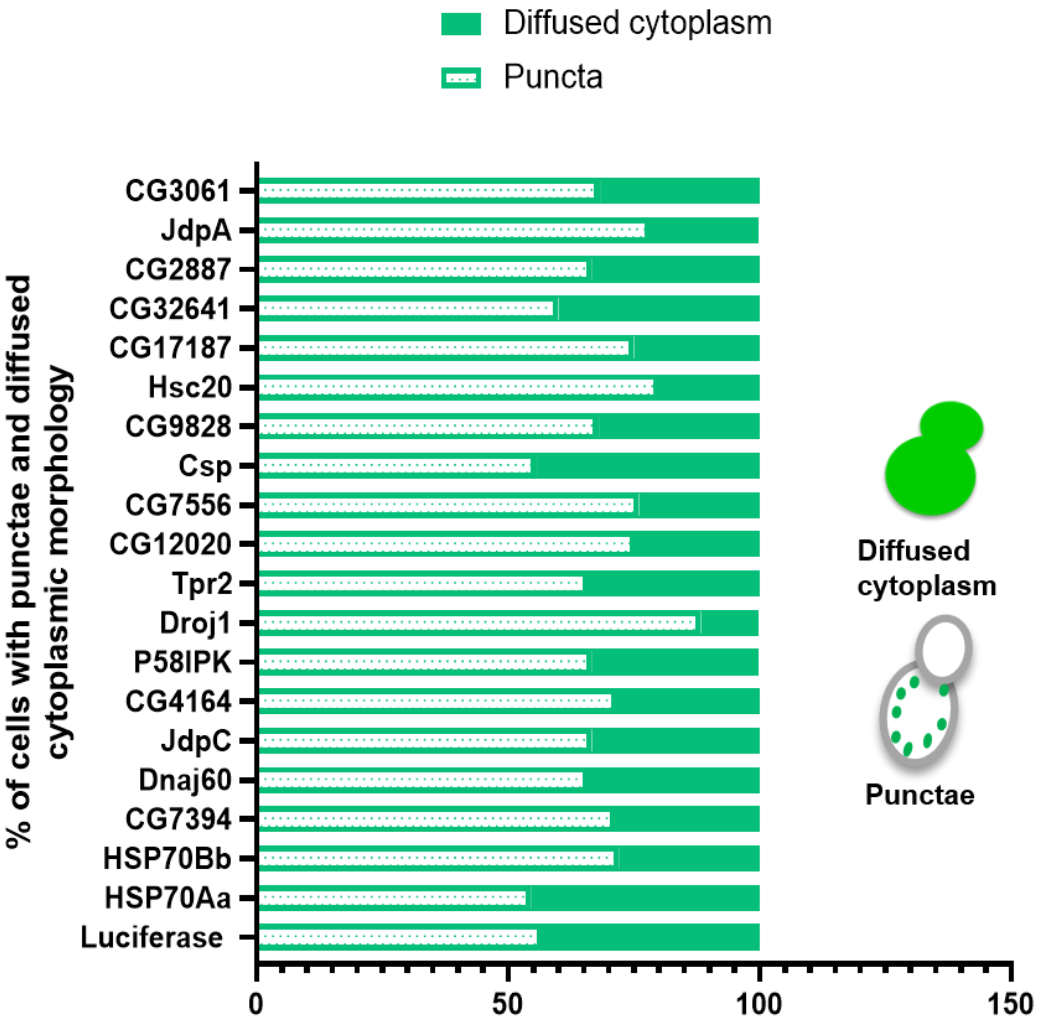
Diffused cytoplasm
Puncta
% of cells with punctae and diffused cytoplasmic morphology
CG3061
JdpA
CG2887
CG32641
CG17187
Hsc20
CG9828
Csp
CG7556
CG12020
Tpr2
Droj1
P58IPK
CG4164
JdpC
Dnaj60
CG7394
HSP70Bb
HSP70Aa
Luciferase
0
50
100
150
Diffused cytoplasm
Punctae

Fig 1f

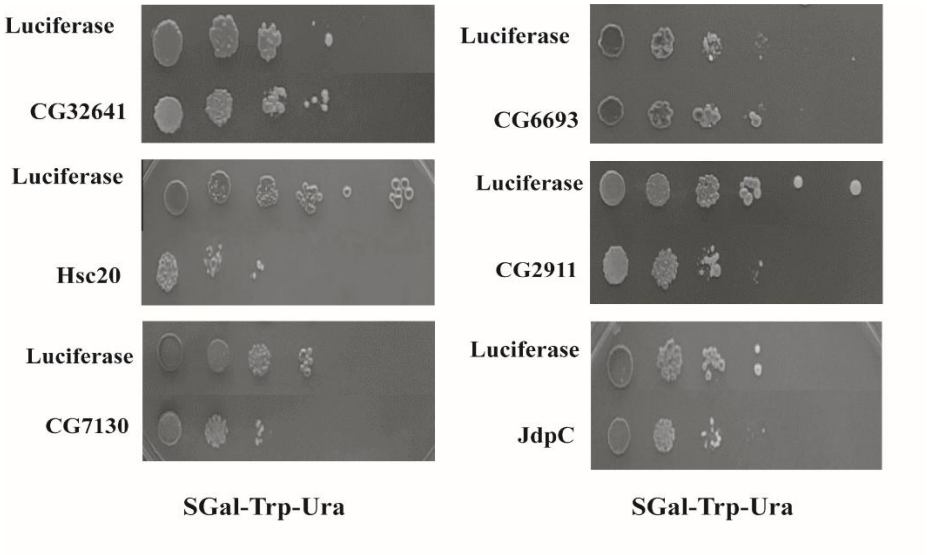
Luciferase
CG32641
Luciferase
CG6693
Luciferase
Hsc20
Luciferase
CG2911
Luciferase
CG7130
Luciferase
JdpC
SGal-Trp-Ura
SGal-Trp-Ura

1g

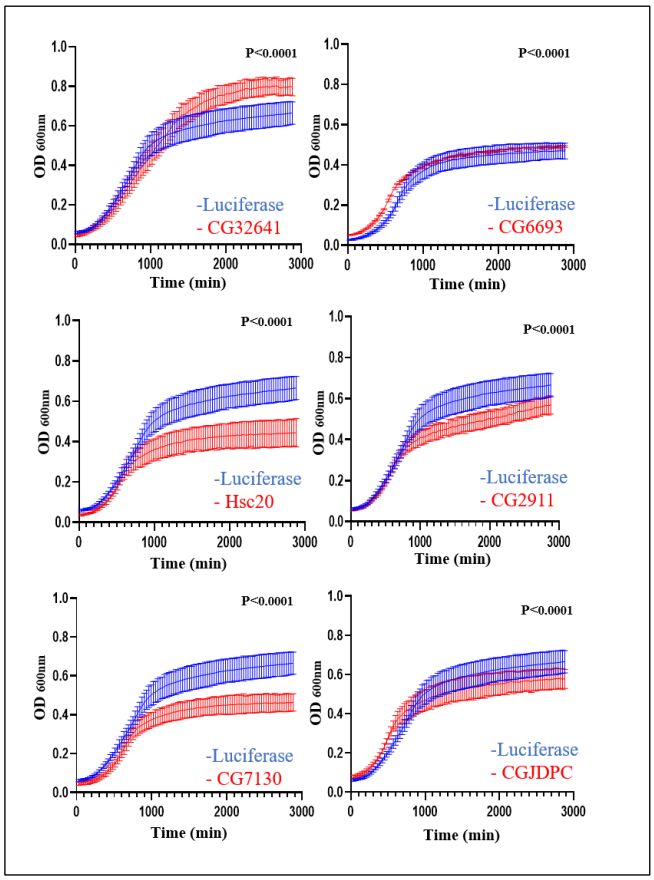
P<0.0001
OD 600nm
Time (min)
-Luciferase
- CG32641
-Luciferase
- CG6693
-Luciferase
- Hsc20
-Luciferase
- CG2911
-Luciferase
- CG7130
-Luciferase
- CGJDPC

1h

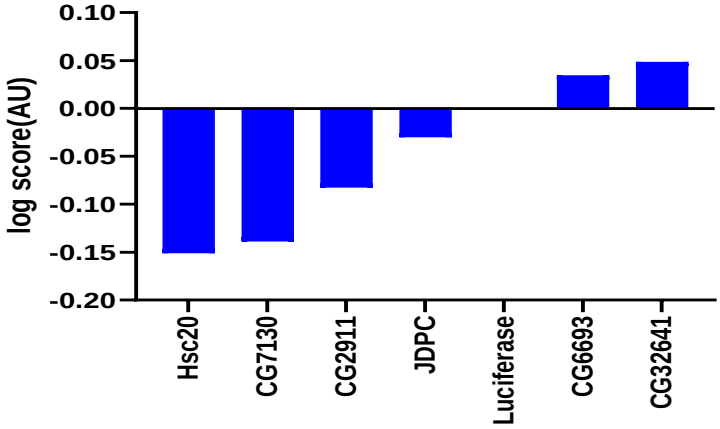
0.10
0.05
0.00
-0.05
-0.10
-0.15
-0.20
log score(AU)
Hsc20
CG7130
CG2911
JDPC
Luciferase
CG6693
CG32641

1i

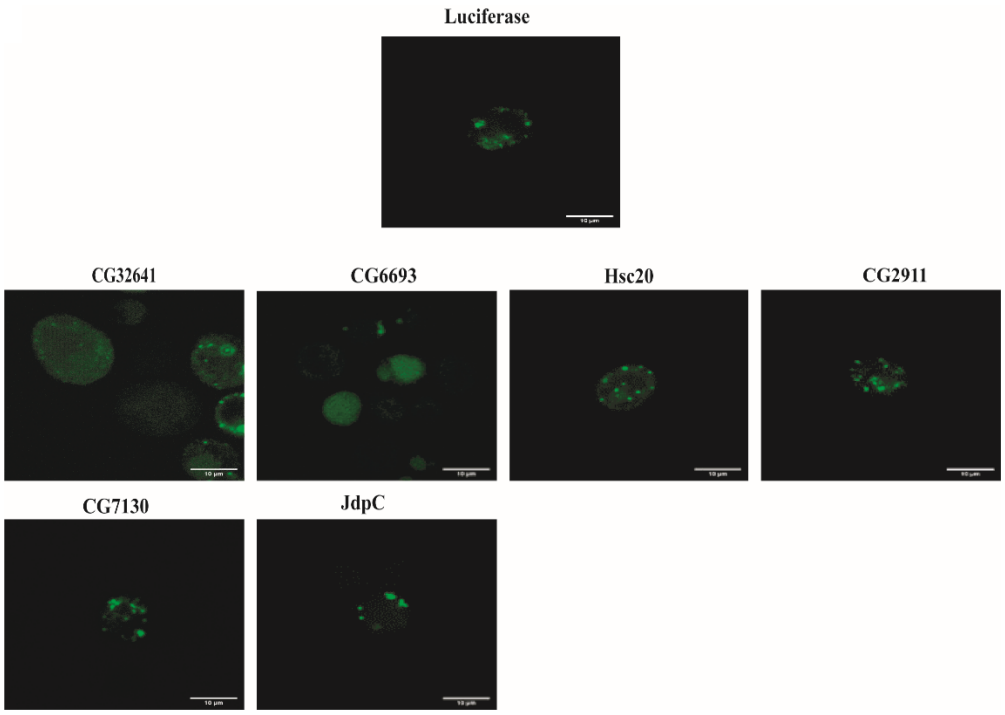
Luciferase
CG32641
CG6693
Hsc20
CG2911
CG7130
JdpC

1j

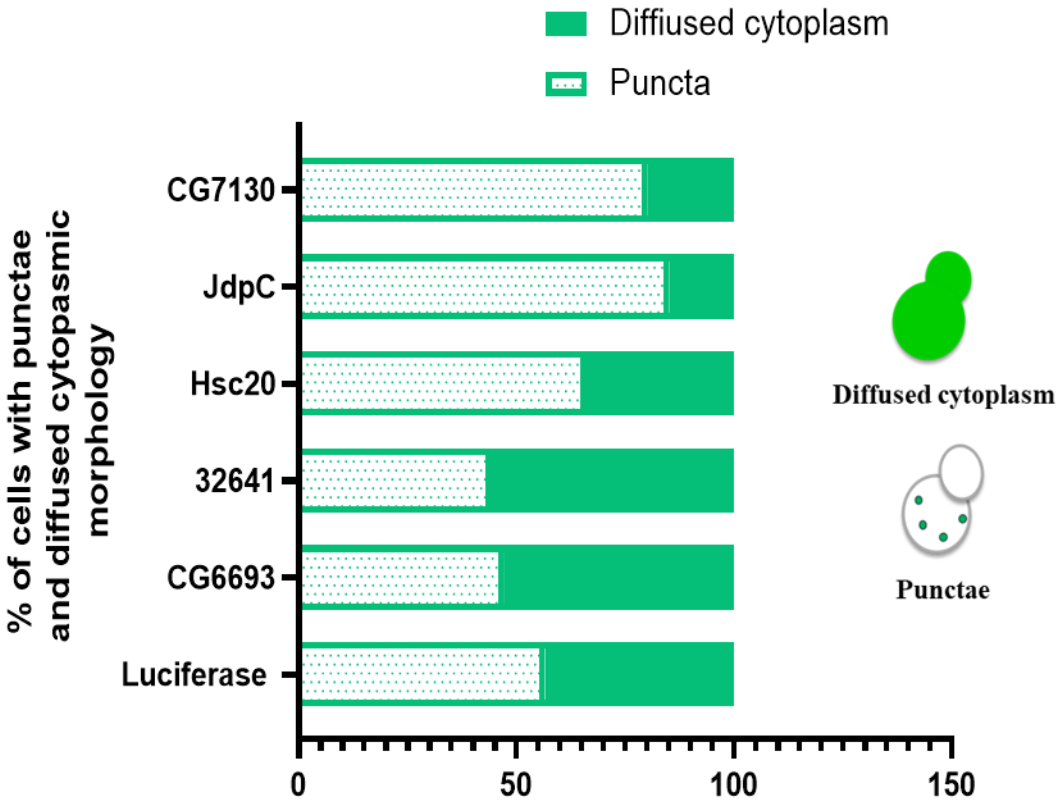
Diffiused cytoplasm
Puncta
% of cells with punctae and diffused cytopasmic morphology
CG7130
JdpC
Hsc20
32641
CG6693
Luciferase
0
50
100
150
Diffused cytoplasm
Punctae

Fig 2f

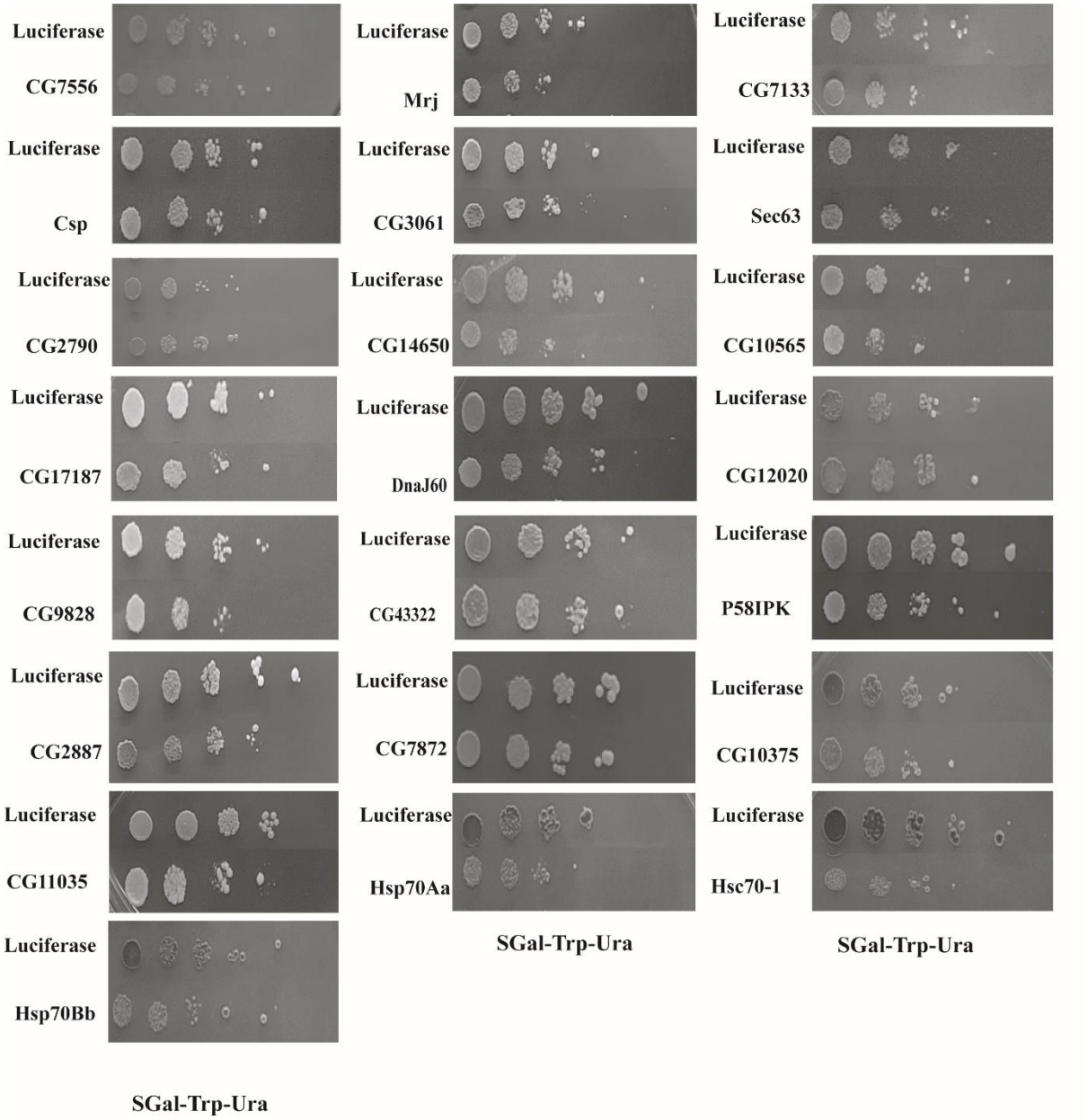
Luciferase
CG7556
Luciferase
Csp
Luciferase
CG2790
Luciferase
CG17187
Luciferase
CG9828
Luciferase
CG2887
Luciferase
CG11035
Luciferase
Hsp70Bb
SGal-Trp-Ura
Luciferase
Mrj
Luciferase
CG3061
Luciferase
CG14650
Luciferase
DnaJ60
Luciferase
CG43322
Luciferase
CG7872
Luciferase
Hsp70Aa
SGal-Trp-Ura
Luciferase
CG7133
Luciferase
Sec63
Luciferase
CG10565
Luciferase
CG12020
Luciferase
P58IPK
Luciferase
CG10375
Luciferase
Hsc70-1
SGal-Trp-Ura

2g

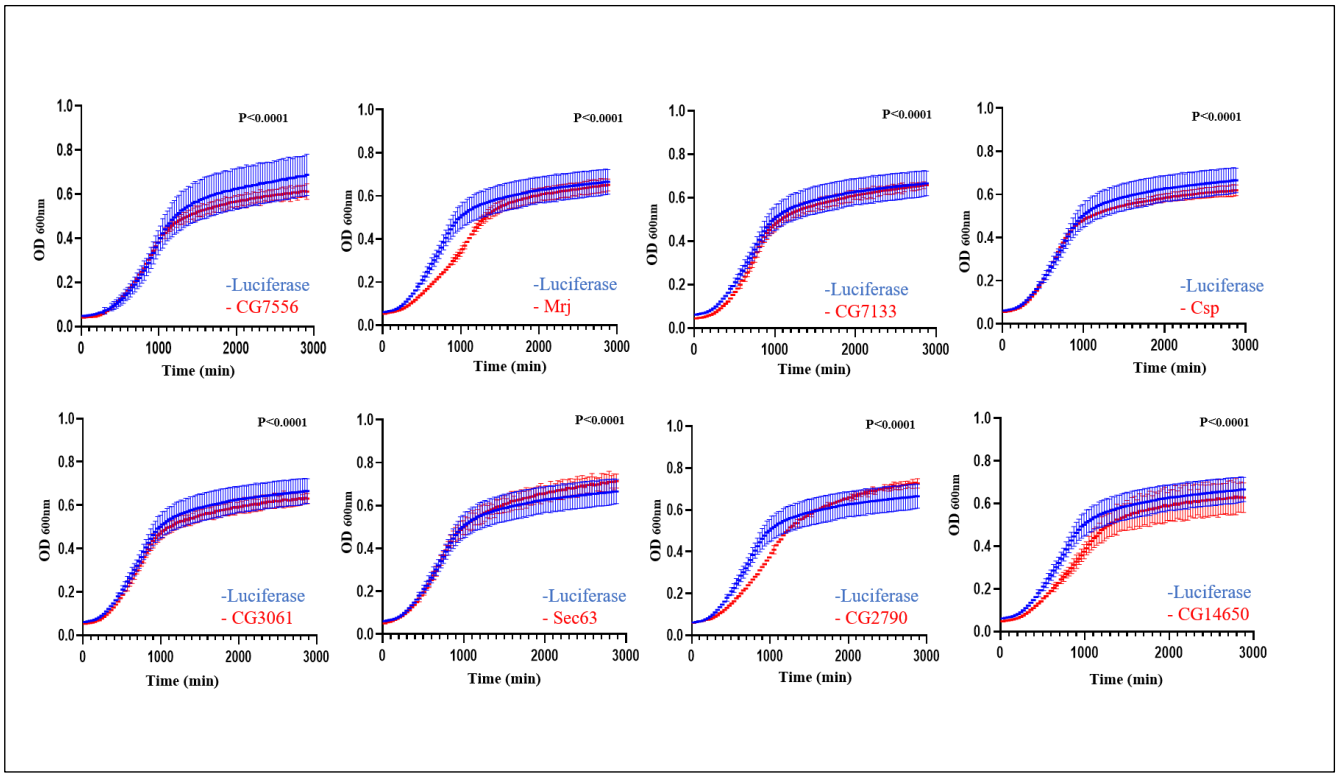
P<0.0001
-Luciferase
- CG7556
-Luciferase
- Mrj
-Luciferase
- CG7133
-Luciferase
- Csp
-Luciferase
- CG3061
-Luciferase
- Sec63
-Luciferase
- CG2790
-Luciferase
- CG14650
OD 600nm
Time (min)

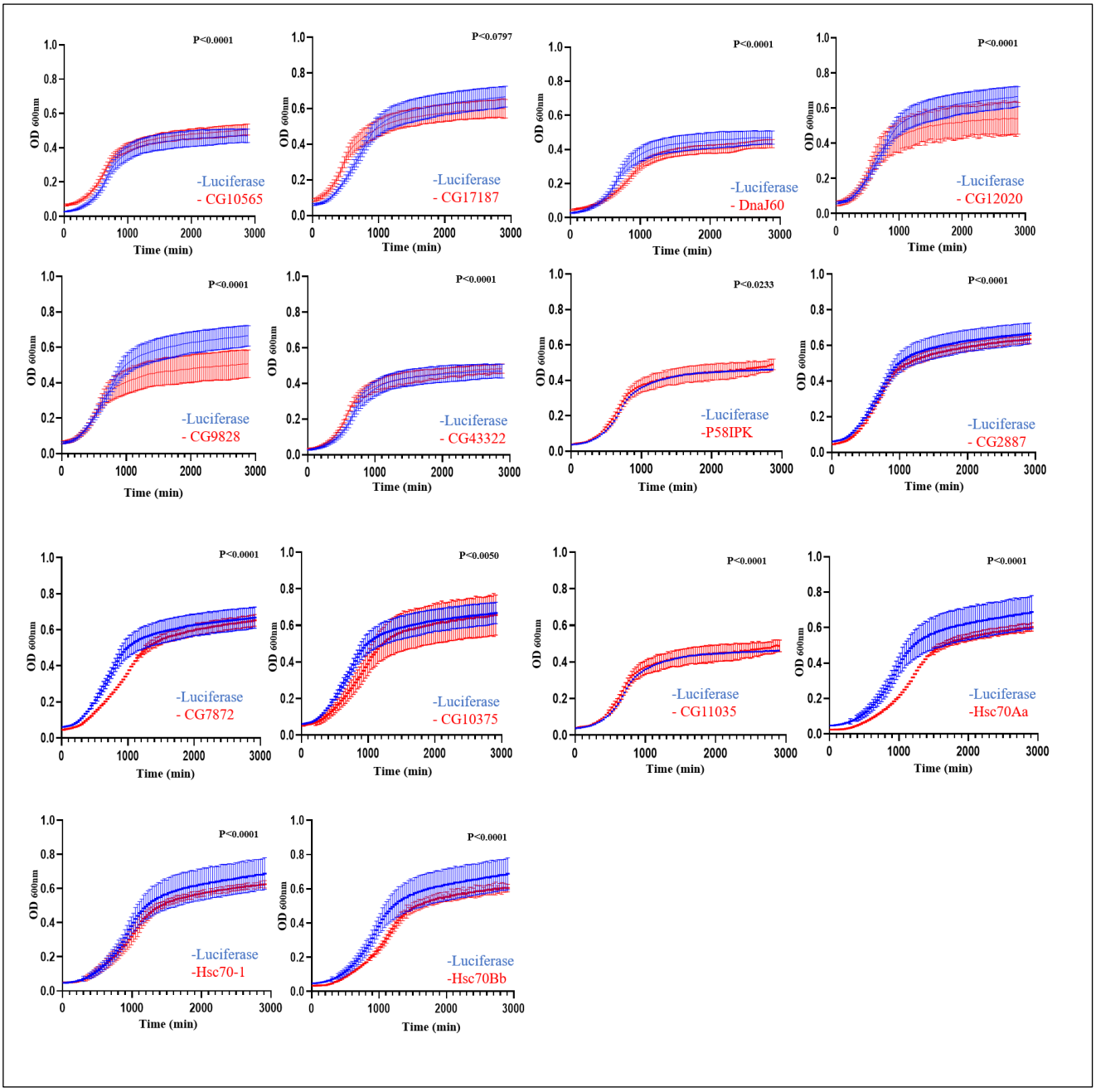
P<0.0001
P<0.0797
P<0.0233
P<0.0050
-Luciferase
- CG10565
-Luciferase
- CG17187
-Luciferase
- DnaJ60
-Luciferase
- CG12020
-Luciferase
- CG9828
-Luciferase
- CG43322
-Luciferase
-P58IPK
-Luciferase
- CG2887
-Luciferase
- CG7872
-Luciferase
- CG10375
-Luciferase
- CG11035
-Luciferase
-Hsc70Aa
-Luciferase
-Hsc70-1
-Luciferase
-Hsc70Bb
OD 600nm
Time (min)

2h

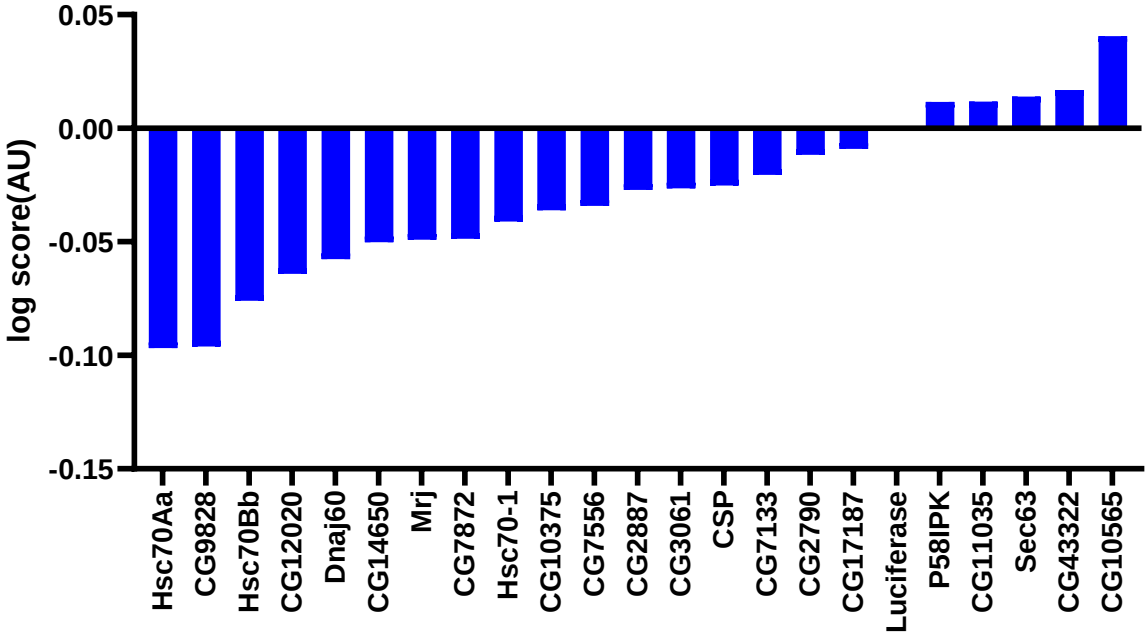
0.05
0.00
-0.05
-0.10
-0.15
log score(AU)
Hsc70Aa
CG9828
Hsc70Bb
CG12020
Dnaj60
CG14650
Mrj
CG7872
Hsc70-1
CG10375
CG7556
CG2887
CG3061
CSP
CG7133
CG2790
CG17187
Luciferase
P58IPK
CG11035
Sec63
CG43322
CG10565

2i

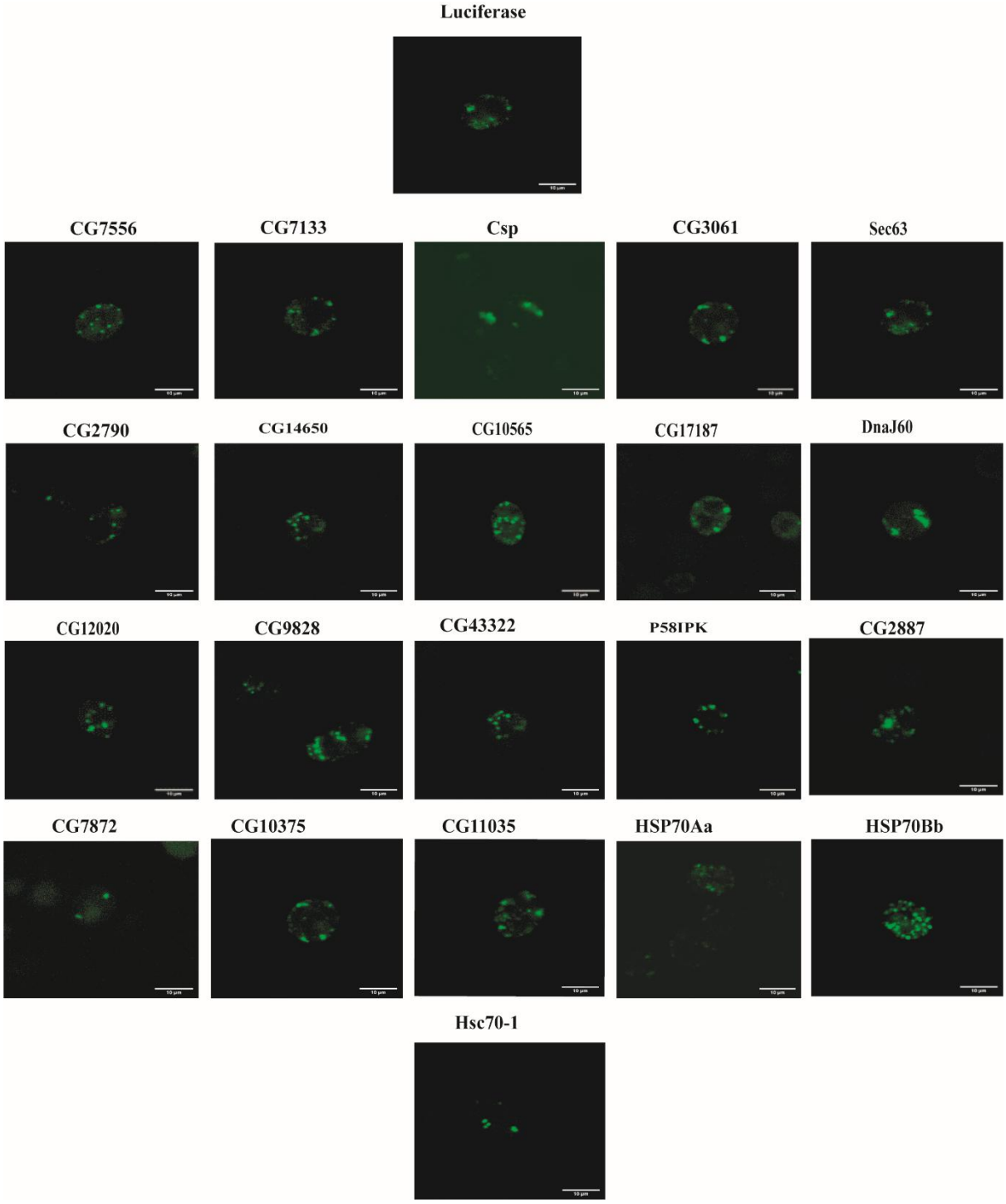
Luciferase
CG7556
CG7133
Csp
CG3061
Sec63
CG2790
CG14650
CG10565
CG17187
DnaJ60
CG12020
CG9828
CG43322
P58IPK
CG2887
CG7872
CG10375
CG11035
HSP70Aa
HSP70Bb
Hsc70-1

2j

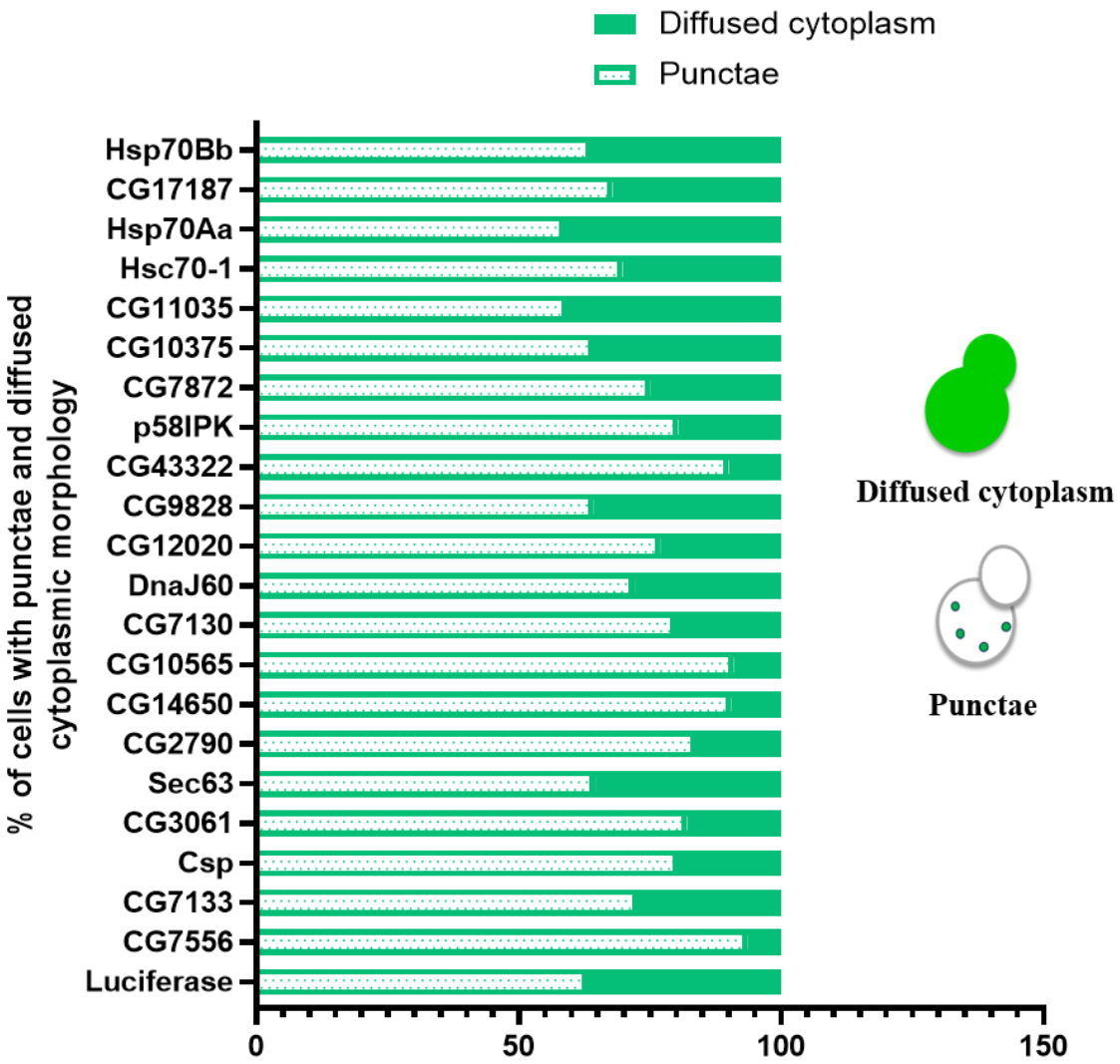
Diffused cytoplasm
Punctae
% of cells with punctae and diffused cytoplasmic morphology
Hsp70Bb
CG17187
Hsp70Aa
Hsc70-1
CG11035
CG10375
CG7872
p58IPK
CG43322
CG9828
CG12020
DnaJ60
CG7130
CG10565
CG14650
CG2790
Sec63
CG3061
Csp
CG7133
CG7556
Luciferase
0
50
100
150
Diffused cytoplasm
Punctae